Regional Assessment and Uncertainty Analysis of Carbon and Nitrogen Balances at cropland scale using the ecosystem model LandscapeDNDC

Odysseas Sifounakis[1], Edwin Haas[2], Klaus Butterbach-Bahl[2,3] and Maria P. Papadopoulou[1]

[1] Laboratory of Physical Geography and Environmental Impacts, School of Rural, Surveying and Geoinformatics Engineering, National Technical University of Athens, Athens, 15780, Greece

[2] Institute of Meteorology and Climate Research (IMK-IFU), Karlsruhe Institute of Technology, Kreuzeckbahnstr. 19, D-82467 Garmisch-Partenkirchen, Germany

[3] Department of Agroecology - Center for Landscape Research in Sustainable Agricultural Futures - Land-CRAFT, Aarhus University, Aarhus, 8000, Denmark

Correspondence to: Edwin Haas (edwin.haas@kit.edu)

Abstract

The assessment of cropland carbon and nitrogen (C & N) balances play a key role to identify cost effective mitigation measures to combat climate change and reduce environmental pollution. In this paper, a biogeochemical modelling approach is adopted to assess all C & N fluxes in a regional cropland ecosystem of Thessaly, Greece. Additionally, the estimation and quantification of the modelling uncertainty in the regional inventory are realized through the propagation of parameter distributions through the model leading to result distributions for modelling estimations. The model was applied on a regional dataset of approximately 1000 polygons deploying model initializations and crop rotations for the 5 major crop cultivations and for a timespan of 8 years. The full statistical analysis on modelling results (including the uncertainty ranges given as ± values) yields for the C balance carbon input fluxes into the soil of 12.4 ± 1.4 tons C ha^{-1} yr^{-1} and output fluxes of 11.9 ± 1.3 tons C ha^{-1} yr^{-1}, with a resulting average carbon sequestration of 0.5 ± 0.3 tons C ha^{-1} yr^{-1}. The averaged N influx was 212.3 ± 9.1 kg N ha^{-1} yr^{-1} while outfluxes were estimated on average of 198.3 ± 11.2 kg N ha^{-1} yr^{-1}. The net N accumulation into the soil nitrogen pools was estimated to 14.0 ± 2.1 kg N ha^{-1} yr^{-1}. The N outflux consist of gaseous N fluxes composed by N_2O emissions 2.6 ± 0.8 kg N_2O-N ha^{-1} yr^{-1}, NO emissions of 3.2 ± 1.5 kg NO-N ha^{-1} yr^{-1}, N_2 emissions 15.5 ± 7.0 kg N_2-N ha^{-1} yr^{-1} and NH_3 emissions of 34.0 ± 6.7 kg NH_3-N ha^{-1} yr^{-1}, as well as aquatic N fluxes (only nitrate leaching into surface waters) of 14.1± 4.5 kg NO_3-N ha^{-1} yr^{-1}, N fluxes of N removed from the fields in yields, straw and feed of 128.8 ± 8.5 kg N ha^{-1} yr^{-1}.

KEYWORDS: greenhouse emissions, ecosystem modelling, cropland carbon and nitrogen balance, inventory, Thessaly region, LandscapeDNDC

Graphical abstract: Result distributions of all nitrogen fluxes with means and medians

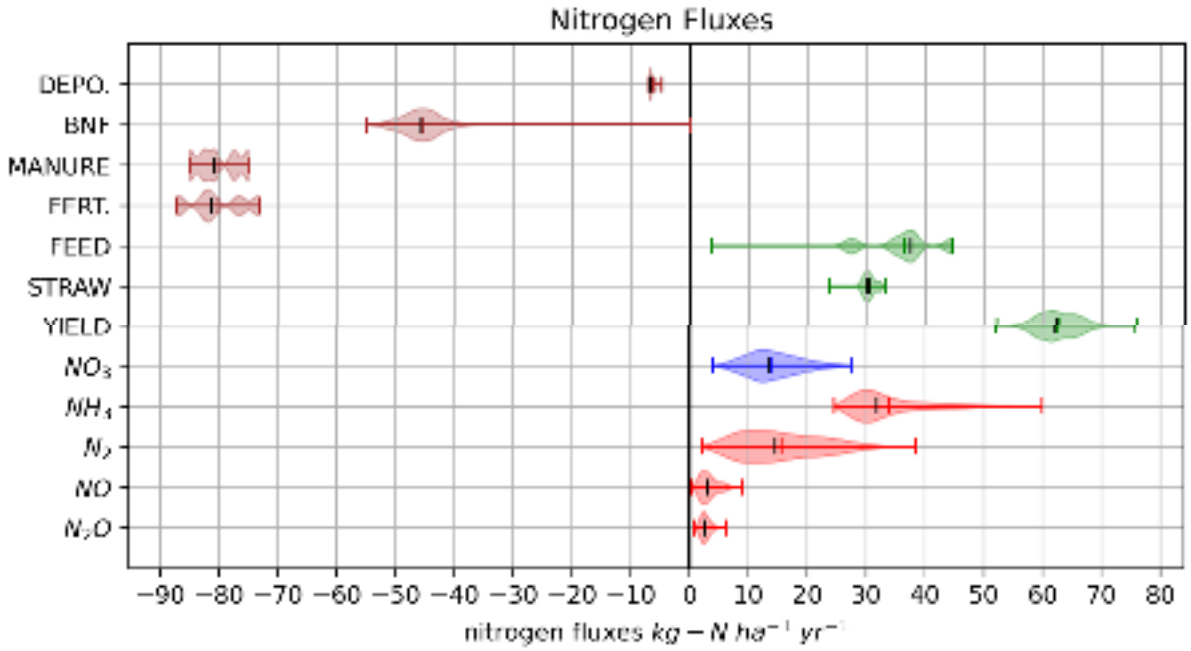

1 Introduction

Food security as well as the agricultural productivity depend to a major extend on the applied nitrogen (N) fertilizers (Klatt et al., 2015a). Worldwide, the N fertilizer use for the years 1960 to 2005 has increased from 30 to 154 million tons (IFADATA, 2015). In Europe, the increase of yields in arable land and grassland systems was 45-70% since 1950 (EFMA, 2009) due to the agricultural production systems intensification. Excessive use of N fertilizers, though beneficially affecting the yield, could cause a harmful impact to the environment, e.g. increased gaseous emissions and aquatic fluxes of nitrous oxide (N_2O) to the atmosphere and leaching of nitrate (NO_3) into water bodies (Erisman et al., 2011; Galloway et al., 2013; Kim et al., 2015) The N_2O poses a twofold environmental threat. From the one hand, it is a strong greenhouse gas with a warming potential of 300 times greater (in a 100-year time period) than carbon dioxide (CO_2) and from the other hand, it is a major driver of ozone depletion in stratosphere (Ravishankara et al., 2009). The fertilizer use aiming at the increase of the agricultural production is the most crucial anthropogenic source of atmospheric N_2O, which at present contributes for approximately 45% of total anthropogenic N_2O emissions on a global scale (Jones et al., 2014). Because of the global population growth and thus a growing food and feed demand (Godfray et al., 2010), the fertilizer use will probably increase. Consequently, the prediction of the current business-as-usual scenarios show doubled anthropogenic N_2O emissions by the year 2050 (Davidson and Kanter, 2014). The European countries have recently set up bilateral agreements in order to reduce N_2O emissions from cultivated crop lands (EU-Commission, 2014). Similarly, the European Nitrates Directive (EU-Commission, 2019; Musacchio et al., 2020) aims at NO_3 leaching reduction to water bodies to avoid both an increase of eutrophication (Camargo and Alonso, 2006) and drinking water pollution. Because of the hazardous N_2O and NO_3 effects, agricultural systems are necessary to be evaluated for their profitability and productivity as well as for their impacts to the environment.

The N_2O and NO_3 production and consumption in agricultural lands are regulated to a large extend by N plant uptake and, also, the microbial processes of denitrification and nitrification (Butterbach-Bahl et al., 2013). The factors controlling both the microbial metabolism and plant

N uptake are a) soil conditions (Butterbach-Bahl et al., 2013) and b) cultivation management practices e.g. crop rotation, fertilizing amount and timing, and ploughing (Smith et al., 2008). In order to reach a minimization of the environmental footprint of agricultural production while securing the global food security (Garnett et al., 2013), it is mandatory to tighten the N cycling on intensified agricultural systems e.g., by harmonizing N demand of crops with soil N availability by N fertilization.

Full nitrogen balance inventories provide a comprehensive understanding of the different N input and output fluxes within an arable system to the scientific community, farmers and policy makers. The assessment of the N balance is essential to optimize nitrogen use and production and minimize environmental impact and pollution. Especially policy making and regulatory bodies require accurate and robust information on all different nitrogen fluxes to develop effective strategies in agricultural N management. Up to now, our understanding of N cycling in arable land lacks observations of the full N balance as only few studies tried to quantify the total N balance of agricultural systems, e.g. (Zistl-Schlingmann et al., 2020) using stable isotope techniques or (Schroeck et al., 2019) using process based modelling.

A recent opinion paper by a large group of leading scientists Grosz et al., (2023) in the field of process based ecosystem modelling identified the lack of knowledge on the full N balance and "the scarcity of complete modeled N balances in the literature stems from the reluctance of the scientific community to support the publication of unvalidated modeled results, especially given that the simulation results of these neglected N pools and fluxes may be unrealistic. This this self-censorship of authors has resulted in a missed opportunity to share knowledge and improve our understanding of modeled processes."

Grosz et al., (2023) conclude that "including the entire N balance and related should become standard when publishing the results of N model studies." Grosz et al., (2023) emphasize that this would allow to assess the robustness of modelled N fluxes and full N balances, and to illustrate the diversity and uncertainty of the different process based modeling approaches, e.g. modelling denitrification processes in soils.

In this analysis, the process-based bio-geochemical model LandscapeDNDC (Haas et al., 2013) was applied to the agricultural cropland systems in the region of Thessaly (Greece). The objective of our study was threefold:

i) Assesing and reporting the cropland C and N balance including all associated fluxes such as e.g. CO_2, N_2O and NH_3 emissions, NO_3 leaching as well as the soil carbon stock changes as demanded by Grosz et al., (2023).

ii) Increasing the robustness and trustworthiness of the balance modelling by assesing and quantifying the modelling uncertainty of the simulated C and N balance and flux estimations as requested before by the IPCC (IPCC, 2019)

iii) Presenting a regional uncertainty assessment methodology for C and N cycling to advance the balance modelling by propagating 500 joint parameter and input data distributions through the model (each representing a full regional C and N balance inventory simulation) yielding regional result distributions for any modelling estimations.

2 Material and Methods

2.1 Model description

LandscapeDNDC is a modular process-based ecosystem model for simulating the bio-geochemical change of C and N in croplands, forest and grassland systems at both site and regional scale. The modules combined are about plant growth, micro-meteorology, water cycling, physico-chemical-plant and microbial C and N cycling and exchange processes with atmosphere and hydrosphere of terrestrial ecosystems. LandscapeDNDC is a generality of the plant development and soil biogeochemistry of the agricultural DNDC and Forest-DNDC (Li, 2000). There is a successful application of earlier model versions in a number of studies, e.g. water balance (Grote et al., 2009; Holst et al., 2010), plant growth (Cameron et al., 2013; Werner et al., 2012), NO_3 leaching (Kim et al., 2015; Thomas et al., 2016) and soil respiration and gas emission trace (Chirinda et al., 2011; Kraus et al., 2014; Molina-Herrera et al., 2015).

For the initialization of LandscapeDNDC physical and chemical site-specific soil profile information is used (specified for different soil depths): Soil organic carbon (SOC) and nitrogen (SON) content, soil texture (clay, sand and silt content), of the plant growth and soil biogeochemistry, bulk density, pH value, saturated hydraulic conductivity, field capacity and wilting point. Daily or hourly climate data of air temperature (max, min and average), N deposition, precipitation, and atmospheric CO_2 concentration are used in LandscapeDNDC in combination with agricultural management practices e.g. crop planting and harvesting, fertilizing (synthetic and organic) or feed cutting and tilling are used to drive LandscapeDNDC simulations. Regarding fertilization management three types of mineral fertilizers, i.e. urea, compound fertilizers based on NH_4 and NO_3 as well as organic amendments, i.e. green manure, farmyard manure, slurry, straw, bean cake and compost are currently considered. The growth of crops and grasses is similar to the DNDC approach using two major parameters that describe seasonal plant development (cumulative temperature degrees days) and maximum reachable biomass under optimum conditions (Li, 2000) while daily growth limitations due to water and nutrient availability are considered. Model parameters describing soil and vegetation characteristics are obtained from an external parameter library. In LandscapeDNDC, the parameterization of the main cultivated commodity crops in Europe occurs by default parameter sets representing an average plant type while process parameter values for micro-meteorology, water cycle and bio-geochemical processes were obtained from previous validation studies, e.g. (Klatt et al., 2015a; Molina-Herrera et al., 2016; Rahn et al., 2012) proving that the LandscapeDNDC model could be universally applicable for similar conditions.

For all simulations in the current study, site-specific crop parameterizations were derived in a preceding analysis of various site scale simulations and validations of yield characteristics across the region. An overview of the crops cultivated at the different study sites and detailed information on specific crop rotations used to simulate crop growth are provided in Table A2 (supplementary material).

2.2 Case study description and input data

The region of Thessaly is located in Central Greece covering a total area of 14 000 Km^2, where 5000 Km^2 is lowland and approx. 2300 Km^2 and 6500 Km^2 are semi-mountainous and mountainous land respectively. The plain of Thessaly is considered to be among the largest agricultural land of the country (Kalivas et al., 2001) accounting for almost 410 000 ha, of which about 370 000 ha is arable land where almost 80% is covered by annual and 10% by perennial crops (ELSTAT, 2012). The crop/plant production of the region is around 14.2% (ELSTAT, 2012) of the total production of the country (2^{nd} in Greece).

Soil input data for the region was available from the European Project Nitro Europe IP (Sutton et al., 2013) based on the European Soil Database (ESDB v2.0, 2004) containing, soil type and soil profile description of bulk density, SOC content, texture (sand, silt clay), pH value, stone fraction, saturated hydraulic conductivity, wilting point and water-holding capacity in various soil strata (Cameron et al., 2013). A regional soil dataset for the area of interest contained about 1500 spatial polygons out of which approximately 1000 covered the cultivated cropland that was finally simulated. The climate data for the regional simulations was derived at polygon level from gridded ERA5 climate data for Greece.

2.3 Agricultural Management and model input data processing

The total cultivated area and the respective yields for the years 2010 to 2016, used in the current analysis were obtained from the Hellenic Statistical Authority (ELSTAT). Moreover, data associated with the animal capital for the respective years was also provided (ELSTAT) in order to estimate the annual manure production distributed in the region however no data is available on whether and how much of the manure is used in croplands. For the water management, the percentage of irrigated and non-irrigated land (estimated to almost 50% for each case) was also given (ELSTAT) while indicative sets of irrigation management data were acquired through the River Basin Management Plans of the Special Secretariat for Water, Ministry of Environment and Energy (YPEKA, Portmann et al., 2010). The irrigation water volumes were estimated based on the crops needs and the minimum and maximum quantities

necessary according to literature while using upscaling tools to get the regional values. The fertilization data sets were provided by Fertilizer Producers and Merchandiser Association (FPMA) for the recent years (2010-2016) and are equated to the annual consumed quantities on a national level, scaled down to a regional level based on crop pattern in the Region of Thessaly cultivated land.

In this study, the five main crops maize, wheat, clover, cotton and barley were considered, covering the majority of the cultivated arable land in the region (over 95%) while the remaining cropland was included acquiring the final corrected land/crop coverage. In Table 1 the resulting crop rotation scenarios (R1 - R5) are presented for the evaluation period 2012 - 2016. Note, each rotation sequence (R1 – R5) is shifted in time such that for each year, each crop appears exactly in one rotation. Based on the crop cover contribution in each simulated year the crop rotation contribution factors were estimated and are summarized in Table 2. The management practices were based on the general agricultural practices applied in the region and information provided by farmers.

Table 1. Summary of the crop rotation scenarios (R1- R5) for the region of Thessaly. The crop abbreviations corn, wiwh, clover, cott and wbar refer to maize (food corn and silage maize), winter wheat, clover (legume feed crops s.a. alfalfa or vetch), cotton and winter barley respectively.

year	R1	R2	R3	R4	R5
2012	clover	cotton	wbar	corn	wiwh
2013	cotton	wbar	corn	wiwh	clover
2014	wbar	corn	wiwh	clover	cotton
2015	corn	wiwh	clover	cotton	wbar
2016	wiwh	clover	cotton	wbar	corn

Table 2. Crop cultivation area contribution per year to the aggregation of the five rotations; data constant across the region of Thessaly

Crop Rotation Contribution [% / 100]					
Years	R1	R2	R3	R4	R5
2012	0.15	0.15	0.45	0.11	0.14
2013	0.13	0.29	0.09	0.10	0.39

2014	0.29	0.13	0.10	0.35	0.12
2015	0.15	0.11	0.43	0.16	0.16
2016	0.10	0.36	0.14	0.14	0.25

201

202

203 ## 2.4 Uncertainty analysis

204 As stated in the IPCC 2006 guidelines and updated in 2019, the assessment of uncertainty is
205 considered a major and crucial/mandatory component when compiling regional or national
206 GHG emission inventories (Larocque et al., 2008). The difference in scale in which the model
207 is used results in divergent errors of the C and N dynamics prediction across different climate
208 zones and scales. Thus, uncertainty analysis is a crucial step towards a higher quality decision
209 making process. The sources of uncertainty can vary and are related to a) the initial conditions
210 (starting values), b) the drivers (e.g. climate and crop management data), c) the conceptual
211 model uncertainty and d) the parameter uncertainty of the various processes (Refsgaard et al.,
212 2007; Wang and Chen, 2012).
213 Santabárbara, (2019) performed a Bayesian Model Calibration and Uncertainty Analysis using
214 a Monte Carlo Markov Chain (MCMC) approach targeting uncertainties associated to the data
215 (bulk density, SOC, pH, clay content) of the initial soil conditions, drivers (cropland
216 management such as fertilization/manure rates & timing, harvest & seeding timing, tillage
217 timing) and bio-geochemical process parameterizations.
218 In order to identify the most sensitive process parameters with a reduced number of model
219 simulations, the Morris method (Morris, 1991) obtains a hierarchy of parameters influence on
220 a given output (gaseous N fluxes) and evaluates whether a non-linearity exists or not. (Morris,
221 1991) proposed that this order can be assessed through the statistical analysis of the changes
222 in the model output, produced by the "one-step-at-a-time" changes in “n” number of proposed
223 parameters. Incremental steps of each parameter range, lead to identifying which ones have
224 substantial influences over the concerned results, without neglecting that some effects could

cancel each other (Saltelli et al., 2000), leading to the identification of the 24 most sensitive process parameters (Houska et al., 2017; Myrgiotis et al., 2018b).

Metropolis – Hastings algorithm

The Markov Chain Monte Carlo (MCMC) Metropolis–Hastings algorithm results in numerous parameter sets that approximate the posterior joint parameter distribution by performing a random walk through the space of joint parameter values. This probability evaluation of the data obtained from each step leads to the update of the initial uniform parameter distributions. Bayes' formula relating conditional probabilities may become a powerful and practical computational tool when combined with Markov chain processes and Monte Carlo methods, so-called Markov Chain Monte Carlo (MCMC). A Markov chain is a special type of discrete stochastic processes wherein the probability of an event depends only on the event that immediately precedes it. Integrating parameters (θ) and observation data (D) into Bayes' rule results in the formula:

$$P(\theta|\mathrm{D}) = \frac{P(\mathrm{D}\,|\,\theta) * P(\theta)}{P(\mathrm{D})} \qquad 2.1$$

where $P(\mathrm{D}\,|\,\theta)$, the probability of the data, is used to obtain the probability of these parameters updated by the data: $P(\theta|\mathrm{D})$ where the evidence is computed as:

$$P(D) = \int likelyhood \cdot prior \cdot d\theta \qquad 2.2$$

where $P(D)$ can be numerically approximated with the aforementioned MCMC method (Robert and Casella, 2011).

The method uses prior knowledge concerning the sources of the model uncertainty to obtain a narrowed posterior distribution for each one of the sources. By propagating the parameter distributions through the model, the overall uncertainty in the model results can be quantified.

In a previous study by Santabárbara, (2019), an extensive sensitivity analysis on all soil bio-geochemical process parameters, soil initial data and arable management data was performed identifying the 24 most sensitive process parameters (listed in supplementary material), the most sensitive soil initial data (soil profile data on bulk density, soil organic carbon content, pH value) and the most sensitive management information (fertilization and manure N rates, tilling depth) to aquatic and gaseous N fluxes from arable soils. This was digested in the MCMC simulation sampling a combination of 24 parameter values, 3 values of soil initial data and 3 management information. The sampling of the soil initial data as well as the management data was performed as perturbations to the existing data: For each quantity, a perturbation was sampled individually and applied to all corresponding values in the soil profile or to all years in the management description. The MCMC simulation performed by Santabárbara, (2019) simulated more than 100 000 iterations for various arable sites until the MCMC simulation converged towards a stable combined posterior distribution of parameter values and soil and management input data perturbations. In the current analysis, we have sampled 500 joint parameter / input data perturbation sets from the posterior distributions as reported by Santabárbara, (2019) and we deployed them in simulations (propagation through the model) for the regional inventory leading to 500 inventory simulations. A statistical analysis was, afterwards, applied to estimate the updated regional and temporal result distributions.

2.5 Statistical methods and data aggregation

Regional result aggregation

One full regional inventory simulation consists of 10 individual inventory simulations: Five (5) different crop rotations for irrigated and rain feed conditions were simulated in parallel (see section 2.3). The results of the crop rotations were aggregated according to the crop shares per year (see Table 2) accounting for all effects of the different crops cultivated in the region for irrigated and rain feed conditions. The final inventory simulation results were obtained by considering irrigated versus rain feed water management. The final inventory contains

simulation results aggregated to area weighted yearly means across the total simulation domain accounting for the cropland area of each polygon.

Uncertainty quantification and statistical analysis

A regional aggregation was performed for all 500 uncertainty simulations. All the uncertainty results were finally reported via statistical measures evaluating the 500 regional uncertainty simulation runs reporting mean values, standard deviation, medians and the 25 and 75 interquartile ranges (IQR, Q25 to Q75).

3 Results Analysis and Evaluation

The simulation time span was from 2009 to 2016, while the years 2009 – 2011 were used as spin-up to get all soil C and N pools into equilibrium after the initialization. Therefore, reported simulation results are limited to years 2012 - 2016. The assessment of the regional C and N balances (CB and NB) were obtained - as a consequence of the uncertainty quantification - resulting in distributions and therefore reported by statistical measures such as mean/median or interquartile ranges of the uncertainty ensemble.

3.1 Regional yield simulations and validation

The evaluation of the model performance in estimating the NB and CB components was analyzed based on the comparison of the simulated yield values with the observed yield data provided by the Hellenic Statistical Authority (ELSTAT), averaged for the total simulated period.

Crop yields and feed production

For model validation, datasets of crop yields from Hellenic Statistical Authority (ELSTAT) were used. Table 3 summarizes the aggregated regional crop yields for all the simulated years and the respective mean, median and standard deviation values resulted from the statistical analysis of the simulation results together with the observed yield and feed production provided by the Hellenic Statistical Authority (ELSTAT). Simulated yields consist for cotton of the cotton bolls, clover feed is the total cutting and harvested above ground biomass, for wheat and barley is the grain yield and for maize is accounted grain ear and the stems. Based on the observations, maize appears to be the dominant crop with an average yield of 12 tons ha^{-1}, followed by clover product of 8.4 tons ha^{-1}. The rest of the three crop yields appear to be in the same order of magnitude from 3.3 up to 3.4 tons ha^{-1}.

Table 3. Simulated and observed yields and feed production [tons dry matter ha^{-1}] in the region of Thessaly. All results are based on statistical aggregation across all polygons, rotations, years and finally across all 500 UA inventory simulations. The observed values of dry matter (DM) are provided by the Hellenic Statistical Authority.

Simulated crop yield and feed distributions [tons dry matter ha^{-1}]				Observed [tons dry matter ha^{-1}]
Crops	Median	Mean	standard deviation	Mean
Cotton	3.5	3.3	0.8	3.3
Clover	9.8	9.6	0.6	8.4
Wheat	3.9	3.6	0.9	3.4
Barley	4.7	4.5	1.0	3.3
Maize[1)]	10.2	9.9	1.4	12.0

[1)] Observation data for maize did not distinguish between food corn and silage maize.

Additionally, the simulated average yield of cotton was estimated to 3.3 ± 0.8 tons DM ha^{-1}, wheat to 3.6 ± 0.9 tons DM ha^{-1}, barley 4.5 ± 1 tons DM ha^{-1}, maize 9.9 ± 1.4 tons DM ha^{-1}. As for the feed, the clover was estimated to 9.6 ± 0.6 tons DM ha^{-1}. The average nitrogen use efficiency (NUE) across time and space is 63.29%.

Figure 1 presents the uncertainties of the simulated crop yield across the whole evaluation time span 2012 -2016 both in irrigated and rain feed conditions. As shown, corn shows a much more narrow distribution with a higher median for the irrigated scenario compared to the rain feed while shows the same extreme value variations. To the contrary, winter barley has a wider distribution and slightly higher median for the irrigated scenario and, also, a wider extreme value variation. As for cotton, the distribution appears to be bimodal for the rain feed scenario in which the median is also lower than the one in the irrigated case. In addition, the extreme value variation is wider in the latter case. Finally, for the example of winter wheat irrigated and rain feed scenarios reach the same results.

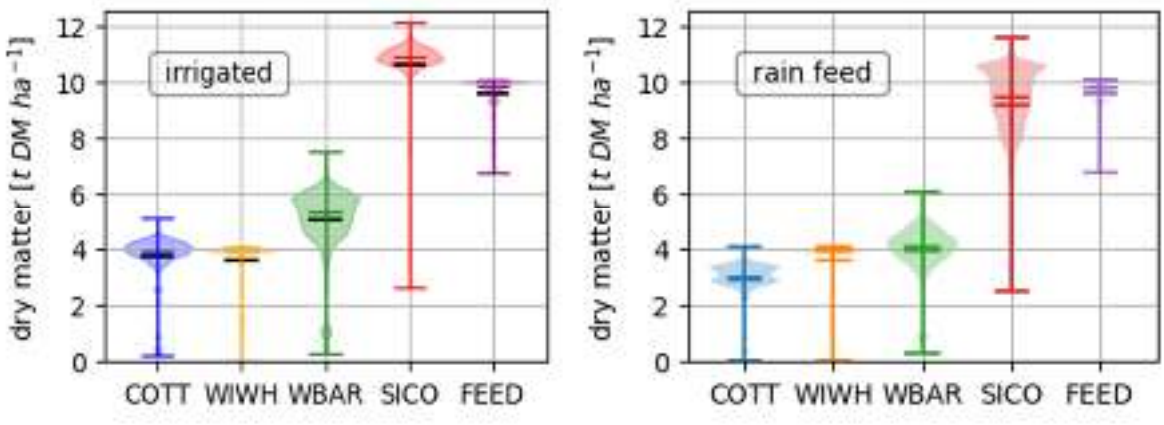

Figure 1. Simulated crop yield uncertainties across the evaluation time span 2012 - 2016 for irrigated and rain feed conditions. Horizontal lines indicate median, mean, maximum and minimum values of the distributions.

3.2 Regional Carbon and Nitrogen Balance

Carbon Balance (CB)

For the CB, Figure 2 presents average C input fluxes into the soil of 12.4 ± 1.4 tons C ha^{-1} yr^{-1} (with inter quartile ranges (IQR) from Q25 to Q75 of 12.1 to 13.2 tons C ha^{-1} yr^{-1}) and output fluxes of 11.9 ± 1.3 tons C ha^{-1} yr^{-1} with IQR from 11.6 to 12.7 tons C ha^{-1} yr^{-1}. The resulting carbon sequestration was estimated to 0.5 ± 0.3 tons C ha^{-1} yr^{-1} with IQR from 0.4 to 0.7 tons C ha^{-1} yr^{-1} (data summarized in Table 4).

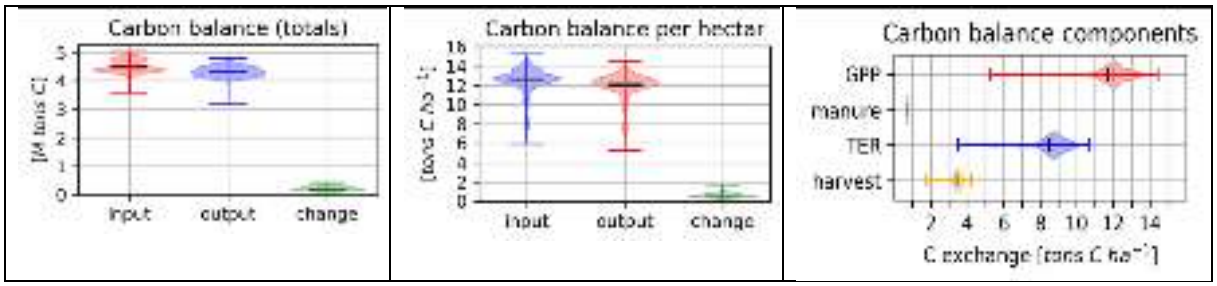

Figure 2. Carbon balance for cropland cultivation for the region of Thessaly: a) Total carbon balance of cropland soils in mio. tons C, b) averaged Carbon Balance in tons C ha^{-1} and c) averaged fluxes across the region and the years 2012-2016. (Positive change equals soil C sequestration).

The input fluxes consist of annual gross primary productivity (GPP) of 11.7 ± 1.4 tons C ha^{-1} yr^{-1} with IQR from 11.4 to 12.4 tons C ha^{-1} yr^{-1} and carbon applied to soils in manure estimated by 0.7 ± 0.001 tons C ha^{-1} yr^{-1} (see Table 4). This compares on the other hand to respirative carbon fluxes from the soil to the atmosphere (TER) of 8.5 ± 1.1 tons C ha^{-1} yr^{-1} with IQR from 8.2 to 9.1 tons C ha^{-1} yr^{-1} and carbon fluxes via exported crop yields and feed (including all straws and removed crop residues) of 3.4 ± 0.3 tons C ha^{-1} yr^{-1} with IQR from 3.4 to 3.6 tons C ha^{-1} yr^{-1}. The aggregation of the carbon fluxes to the regional level of approx. 360 000 ha of cropland results in 4.25 ± 0.20 M tons C yr^{-1} by GPP, 0.25 ± 0.01 M tons C yr^{-1} carbon influx via organic fertilizers compared to 3.08 ± 2.97 M t C yr^{-1} TER and 1.24 ± 0.05 M t C yr^{-1} carbon exports via crop yields and feed production leading to a net carbon sequestration of 0.5 ± 0.3 M tons C ha^{-1} yr^{-1} with IQR from 0.4 to 0.7 M tons C ha^{-1} yr^{-1} (M tons C as Million tons carbon).

*Table 4. **Carbon Balance** (per hectare) Assessment and Uncertainty Analysis of the of cropland cultivation at the region of Thessaly, Greece. [1)] mean; [2)] standard deviation; [3)] median; Interquartile ranges: [4)] Q25: 25 quartile, [5)] Q75: 75 quartile are applied across the 500 values for the quantities in this table; [6)] C-Inputs as the sum of the absolute values of all the input fluxes of the 500 simulations; [7)] C-Outputs as the sum of the absolute values of all the output fluxes of the 500 simulations; [8)] SOC-changes as the difference between the input and output fluxes of each of the 500 simulations.*

	Mean[1)]	Std[2)]	Median[3)]	Q25[4)]	Q75[5)]
	[tons C ha^{-1} yr^{-1}]	[tons C ha^{-1} yr^{-1}]	[tons C ha^{-1} yr^{-1}]	[tons C ha^{-1} yr^{-1}]	[tons C ha^{-1} yr^{-1}]
C-Inputs[6)]	12.4	1.4	12.7	12.1	13.2

C-Outputs[7)]	11.9	1.3	12.2	11.6	12.7
SOC-changes[8)]	0.5	0.3	0.5	0.4	0.7
Input fluxes					
GPP	11.7	1.4	12.0	11.4	12.4
C in manure	0.7	0.0	0.7	0.7	0.7
Output fluxes					
TER	8.5	1.1	8.7	8.2	9.1
Biomass export	3.4	0.3	3.5	3.4	3.6

Nitrogen balance (NB)

In Figure 3 the assessment of the distribution of the NB with the in- and out-fluxes is presented. The averaged nitrogen influx (represented by the uncertainty ensemble mean) per hectare was estimated to 212.3 ± 9.1 kg N ha^{-1} yr^{-1} with IQR from 203.3 to 220.0 kg N ha^{-1} yr^{-1} while nitrogen out-fluxes were estimated in average to 198.3 ± 11.2 kg N ha^{-1} yr^{-1} with IQR from 191.4 to 204.0 kg N ha^{-1} yr^{-1} (Figure 3) leading to a net N accumulation in the soil of 14.0 ± 2.1 kg N ha^{-1} yr^{-1} with IQR from 11.9 to 16.0 kg N ha^{-1} yr^{-1}.

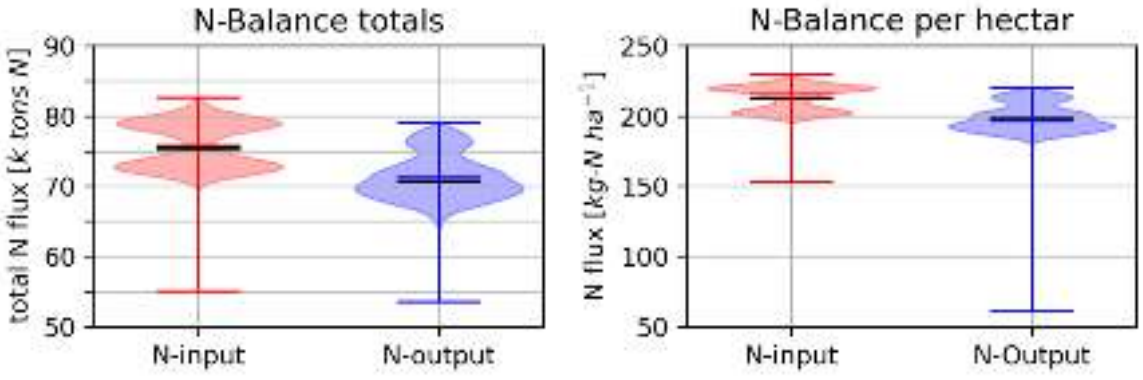

Figure 3. Nitrogen balance for cropland cultivation for the region of Thessaly; a) Total NB in k-tons N and b) averaged NB in kg N ha^{-1}; Data averaged for the years 2012-2016. Horizontal lines indicate mean (red), median and minimum and maximum of the distribution.

*Table 5. Nitrogen Balance (per hectar). Summary of the Assessment and Uncertainty Analysis of the **NB Fluxes** (per hectare) of cropland cultivation of the region of Thessaly, Greece. [1] N-Inputs as the sum of the absolute values of all input fluxes of the 500 simulations; [2] N-Outputs as the sum of the absolute values of all the output fluxes of the 500 simulations; [3] N-stock-changes as the difference between the input and output fluxes of each of the 500 simulations; [4] Gaseous emissions are the sum of N_2O, NO, N_2 and NH_3 fluxes; [5] Aquatic flux is nitrate leaching (NO_3^-).*

	Mean	Std	Median	Q25	Q75
	[kg N ha^{-1} yr^{-1}]	[kg N ha^{-1} yr^{-1}]	[kg N ha^{-1} yr^{-1}]	[kg N ha^{-1} yr^{-1}]	[kg N ha^{-1} yr^{-1}]
N-Inputs[1]	212.3	9.1	215.2	203.3	220.0
N-Outputs[2]	198.3	11.2	196.4	191.4	204.0
N-stock-changes[3]	13.8	2.1	13.7	14.5	12.5
Input fluxes					
N deposition	6.3	0.8	6.8	6.0	6.8
Bio. N fixation	45.6	4.3	45.7	43.7	47.7
N in min. fertilizer	80.2	4.8	81.3	76.6	82.7
N in organic fertilizer	80.2	3.6	80.9	77.5	82.7
Output fluxes					
Gaseous emissions[4]	55.4	8.8	55.1	48.9	61.6
N_2O	2.6	0.8	2.5	2.1	3.1
NO	3.2	1.5	2.9	2.0	4.1
N_2	15.5	7.0	14.6	9.9	20.7
NH_3	34.0	6.7	31.8	29.3	36.9
Aquatic fluxes[5]					
NO_3 leaching	14.1	4.5	13.6	11.0	17.0

The N influx was composed by the input of synthetic fertilizer of 80.2 ± 4.8 kg N ha^{-1} yr^{-1} (IQR 76.6 to 82.7) and organic fertilizer of 80.2 ± 3.6 kg N ha^{-1} yr^{-1} (IQR from 77.5 to 82.7), followed by the biological nitrogen fixation (BNF) via legumes estimated as 45.6 ± 4.3kg N ha^{-1} yr^{-1} (IQR from 43.7 to 47.7) and nitrogen deposition of 6.3 ± 0.8kg N ha^{-1} yr^{-1} (IQR from 6.0 to 6.8). Thus, almost 75% of the nitrogen input influx is related to the fertilization (mineral and organic) whilst the minor part that corresponds to nitrogen fixation and deposition approximates to 25%.

The N outflux consist of gaseous N fluxes of 55.4 ± 8.8 kg N ha^{-1} yr^{-1} (IQR from 48.9 to 61.6), aquatic N fluxes (only nitrate leaching into surface waters was considered) of 14.1 ± 4.5 kg N ha^{-1} yr^{-1} (IQR from 11.0 to 17.0), N fluxes by removed N in yields, straw and feed of 128.8 ± 8.5 kg N ha^{-1} yr^{-1} (IQR of 125.2 to 131.7) (see Figure 4 and Table 5). Based on the aforementioned results all gaseous and aquatic N-fluxes correspond to about 28% and 7% of the N output flux respectively, while the far largest N output flux was N removed in yields, straw and feed representing almost 65% of the N outflux (Figure 4).

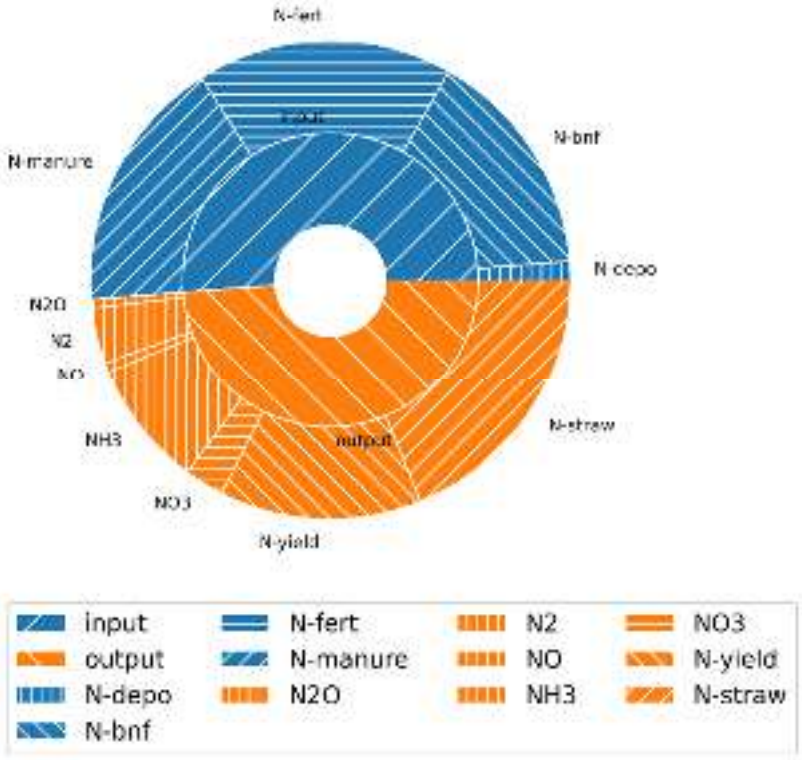

Figure 4. Averaged annual nitrogen balance (inner ring of the pie diagram) and their decomposition into the various components of the N fluxes (outer ring of the pie diagram); (all data summarized in Table 5).

The simulated gaseous fluxes were composed of N_2O emissions estimated to 2.6 ± 0.8 kg N_2O-N ha^{-1} yr^{-1} (IQR from 2.1 to 3.1), NO emissions of 3.2 ± 1.5 kg NO-N ha^{-1} yr^{-1} (IQR from 2.0 to 4.1), N_2 emissions 15.5 ± 7.0 kg N_2-N ha^{-1} yr^{-1} (IQR range from 9.9 to 20.7) and NH_3 emissions of 34.0 ± 6.7 kg NH_3-N ha^{-1} yr^{-1} (IQR from 29.3 to 36.9). Ammonia volatilization represents the largest share (61.48%) of gaseous N losses, with highest densities in the emission distribution between approx. 25 and 35 kg N ha^{-1}, followed by di-nitrogen losses

(28.03%) of gaseous N losses, with a much wider emission variability in the distribution, followed by NO_3 (5.79%) and N_2O (4.7%). Figure 5 shows the overall NB in a waterfall diagram adding up cumulative all in- and out-fluxes illustrating the uncertainty distribution of each flux contributions. The waterfall diagram illustrates the overall outcome of the NB, a N accumulation into the soil as the difference between all out-fluxes minus all in-fluxes.

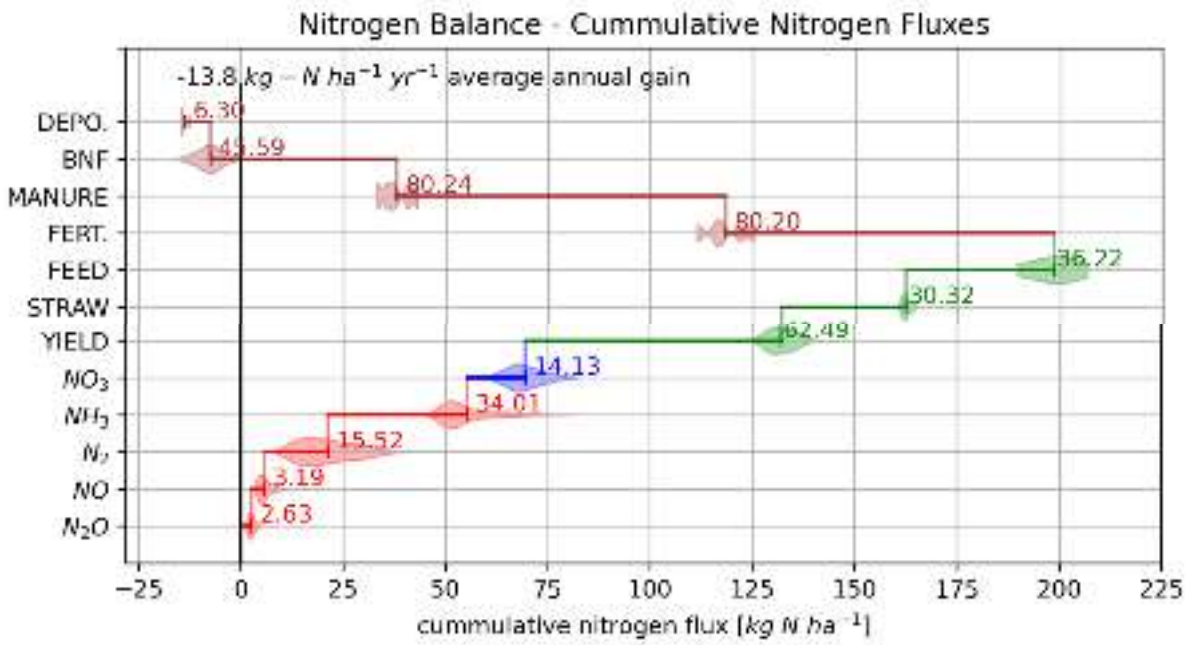

Figure 5. Waterfall representation of the result distributions of the different Nitrogen in- and outfluxes of the cropland cultivation in Thessaly. Vertical lines in the distributions indicate mean values of the corresponding N-flux. Red colors indicate gaseous outfluxes, blue aquatic fluxes, green biomass yield and feed production outfluxes and brown color indicates N influxes such as synth. N-fertilizer, N-Manure, biological N fixation (BNF) and N deposition. The Resulting N sink of the Nitrogen Balance (based on distribution means) is -13.8 kg N ha^{-1} yr^{-1}. (Negative value indicates flux into the soil).

Nitrate leaching mean estimates were 14.1 ± 4.5 kg NO_3-N ha^{-1} yr^{-1} (IQR from 11.0 to 17.0) with a bell-shaped distribution.

Total yield and biomass (straw and feed) N export fluxes were 62.4 ± 4.4 kg N ha^{-1} yr^{-1} with uncertainty ranges from 59.9 to 65.1 consisting of yield N exports (grains and cotton balls) of 30.3 ± 1.7 kg N ha^{-1} yr^{-1} (IQR from 29.6 to 30.9) and for straw and feed N exports of 36.1 ± 6.0 kg N ha^{-1} yr^{-1} (IQR from 34.9 to 37.6). The result distributions for yield N are well bell shaped,

for feed biomass N very moderate bell shaped and well distributed within the bounds and for straw N very sharp within a comparable small interval.

Figure 5 illustrates the cumulative nitrogen fluxes composing the NB as a waterfall diagram considering the mean of each component. The NB results in a net N sink of 13.8 kg N ha^{-1} yr^{-1} (see result distribution in Figure 6) for the region corresponding to an annual carbon sequestration of approx. 0.5 tons C ha^{-1} yr^{-1} as depicted in Figure 2 b) (see also the annual dynamics of the topsoil (30 cm) soil organic carbon and nitrogen distributions in Figure 8).

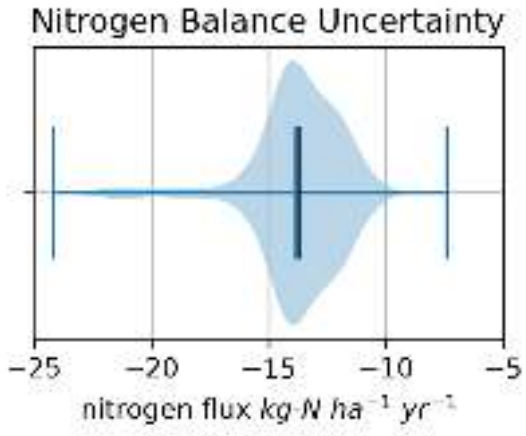

Figure 6. Distribution of the overall Nitrogen Balance of the cropland cultivation in Thessaly: Statistical analysis across all 500 individual NB results of the inventory simulations (mean 13.8 kg N ha^{-1} yr^{-1}, median 13.7 kg N ha^{-1} yr^{-1}) corresponding to the Carbon balance in Figure 2.

Figure 7 and Figure 8 show the dynamics of the annual distribution of the gaseous and aquatic outfluxes as well as the dynamics of the annual distributions of the top soil (30 cm) soil organic carbon and nitrogen pools for the evaluation period 2011 – 2016.

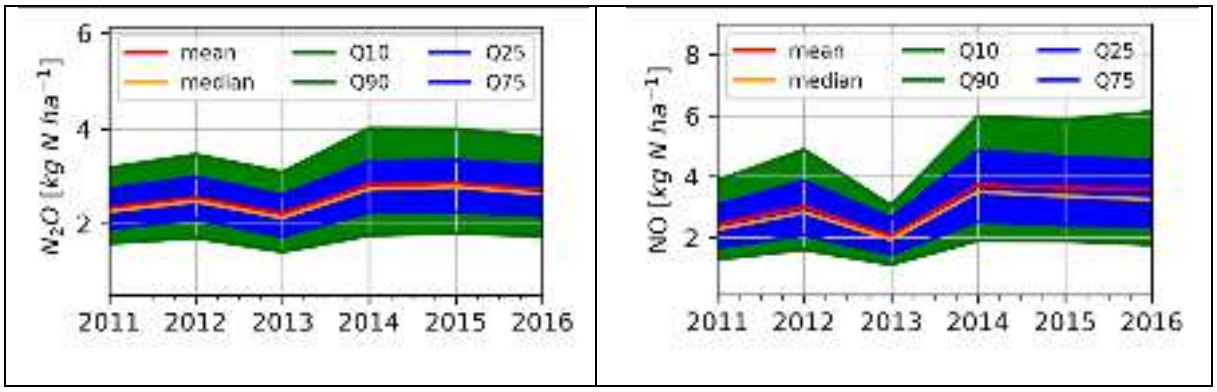

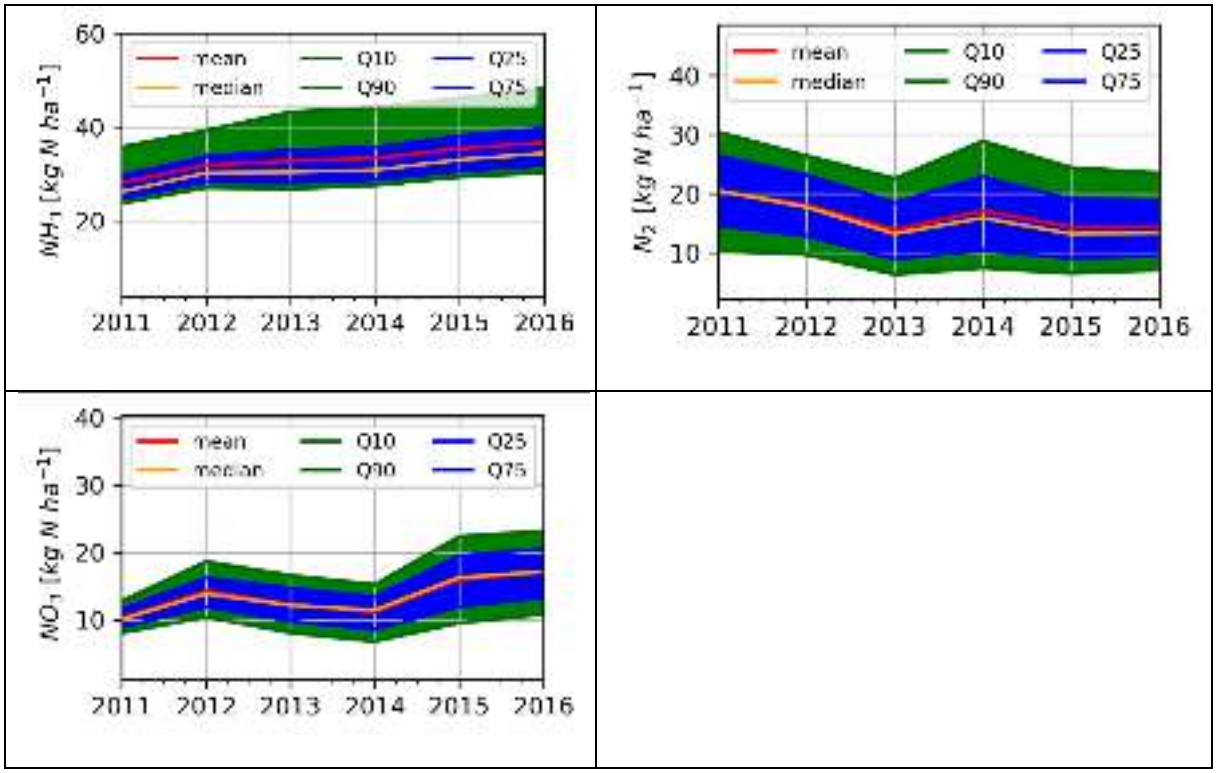

444 *Figure 7. Annual dynamics of the uncertainty distributions of the gaseous (subfigure a) to d)) and aquatic (subfigure*
445 *e)) N outfluxes 2011 – 2016. Uncertainty bandwidth (blue band) defined as the range between the q25 and the q75*
446 *quartile, green band (Q10. to Q90 interval) indicating the variance of the fluxes neglecting the outliners of the*
447 *distribution.*

448

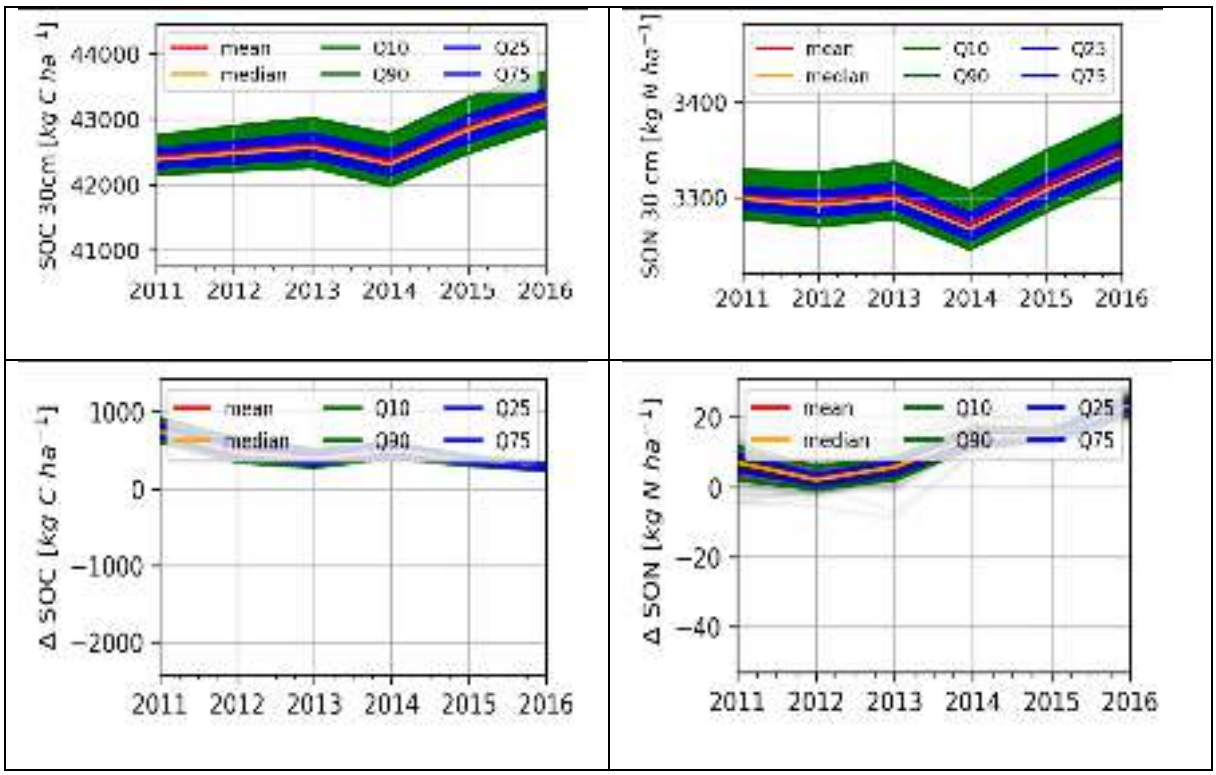

Figure 8. Annual dynamics of the uncertainty distributions of the soil carbon (subfigure a)) and soil organic nitrogen (subfigure b)) and the corresponding dynamics of the uncertainty distributions of the annual change rates of the total soil carbon and nitrogen pools (subfigures c) and d)) respectively.

4 Discussion.

In this study, following the recommendation of Grosz et al., (2023), an assessment of the combined full C and N balance of a regional cropland agroecosystem is reported for the first time using inventory simulations with a process-based ecosystem model. The additional quantification of the associated modelling uncertainty of the balance simulations increase the trustworthiness of the study.

Up to present, process-based modelling studies mainly focus on single site applications e.g. Daycent: (del Grosso et al., 2005; Gurung et al., 2020), APSIM: (Vogeler et al., 2013), CERES-EGC: (Dambreville et al., 2008; Gabrielle et al., 2006; Heinen, 2006; Hénault et al., 2005), CERES-Wheat: (Mavromatis, 2016), DNDC: (Li, 2000), LandscapeDNDC: (Haas et al., 2013; Klatt et al., 2015a; Molina-Herrera et al., 2016; Zhang et al., 2015). Fewer studies deploy models on the regional to national (del Grosso et al., 2005; Kim et al., 2015; Klatt et al., 2015a) or continental to global scale (del Grosso et al., 2009; Franke et al., 2020; Jägermeyr et al., 2021; Smerald et al., 2022; Thompson et al., 2019). All of these studies are subject to criticism stated by Grosz et al., (2023) as they are reporting in general only one specific or a few components of the carbon or nitrogen cycle such as e.g. soil carbon stocks or N_2O emissions, lacking any information on the full C and N balance.

There are only a very few cases where an attempt for regional estimation of the NB has been made. The study reported by Schroeck et al., (2019) is the only previous attempt fulfilling the requirements of Grosz et al., (2023) in reporting the full NB for a large alpine watershed in the Austrian Alps characterized by arable production in the low-lying areas and grassland in the mountains using a process based model. In addition, Lee et al., (2020) tried to estimate nitrogen balances in Switzerland alternating the cropping systems or management practices. There were, also, cases where the regional NB was estimated with the use of nitrogen balance equations (He et al., 2018). Recently, Zistl-Schlingmann et al., (2020) assessed the full N balance of alpine grasslands using the ^{15}N stable isotope techniques.

In order to achieve a more concrete and complete analysis of the CB and NB that could be used for future policy development, an uncertainty analysis is considered as necessary/mandatory. The IPCC guidelines demand for UNFCC reporting the uncertainty quantification of any reported inventory study (IPCC Updated guidelines 2019). Recent publications have reported the deployment of different methods to assess and quantify the various sources of uncertainty in ecosystem modelling. (Klatt et al., 2015b) published a study on the impact of parameter uncertainty on N_2O emissions and NO_3 leaching on the regional scale. (Houska et al., 2017) deployed the GLUE method (Generalized Likelihood Uncertainty Estimation) for the LandscapeDNDC model on a grassland site, other studies such as (Lehuger et al., 2009a; Li et al., 2015; Myrgiotis et al., 2018a) used the Bayesian Model Calibration and Uncertainty Assessment approach, which has been used in the current study as well.

4.1 Yield and feed Production

LandscapeDNDC was validated in a study by Molina-Herrera et al., (2016) on cropland and grassland sites across Europe reporting good agreement in reproducing observed above ground biomass and yield estimates. Similar model performance for the cultivation of commodity crops was reported by (Kasper et al., 2019; Klatt et al., 2015a; Molina-Herrera et al., 2017; R. J. Petersen et al., 2021).

Lyra and Loukas, (2021) used REPIC model to estimate the crop growth/yield production of several crops in the Basin of Almyros, Thessaly. The simulated results were approximately 11 tons ha^{-1} clover, 3.3/3.5 tons ha^{-1} cereals/wheat, 3.8 tons ha^{-1} cotton and 9 tons ha^{-1} maize, being well compared to the results of our research shown in Table 3. The simulated results presented in our study are in line with the results by Voloudakis et al., (2015) simulating cotton production in seven different areas of Greece applying the AquaCrop model. Similar results were reported by (Tsakmakis et al., 2019).

There are few cases in literature concerning yield simulations on a European level. Based on the yield datasets of FAO and EUROSTAT, Ciais et al., (2010a) estimated mean crop yields for the period 1990–1999 at the scale of EU-25 as 6.1 (FAO) and 5.3 (EUROSTAT) tons DM ha^{-1} yr^{-1}, respectively, which corresponds well to results of our study. Haas et al., (2022) estimated with a model ensemble mean for crop yields for EU-27 of 4.41 ± 1.85 tons DM ha^{-1} yr^{-1} for the period 1990–1999. Lugato et al., (2018) estimated cropland yield projections of 4.34 tons DM ha^{-1} yr^{-1} (mean), ranging from 3.69 to 4.90 tons DM ha^{-1} yr^{-1} with the DayCent model for EU-27, comparable to the 6.18 tons DM ha^{-1} yr^{-1} average simulated crop yields of this study. The simulated yields in the current study vary from 3.3 to 9.9 tons DM ha^{-1} yr^{-1} for the cases of cotton and maize respectively.

Higher yield estimates for the region of Thessaly in this study are certainly due to the inclusion of the legume feed crops in the rotations. This argument is supported by a recent meta-analysis by (Lu, 2020) that concluded that on average yield increases of 5.0 to 25% can be expected for various conditions if residues are completely returned to the field as compared to no-residue return systems. Similar results were reported by Fuchs et al., (2020) and Barneze et al., (2020). Following the recommendations of Grosz et al., (2023), our study has reported transparently all major C & N fluxes for the region as being simulated by the model. In our study, we have not calibrated the model against any observations, therefore all simulation results will be discussed versus other modelling results available. As up to now, there is only one comparable modelling study available in literature reporting and discussing the total N balance of a site or region, which we have used to compare our N balance against.

4.2 Carbon and Nitrogen Balance:

Full N balance

At present, the studies of Schroeck et al., (2019) and Lee et al., (2020) are the only to be found by Web of Science under the search key words “nitrogen AND balance AND process AND based AND modelling” reporting a compilation of the nitrogen balance and all associated N

fluxes for a site or region applying a process-based ecosystem model as demanded by Gosz et al (2023).

Leip et al., (2011) reported the first nitrogen balance for Europe following a mixed approach combining the CAPRI (Common Agricultural Policy Regionalised Impact) model (a global economic model for agriculture) with different approaches estimating various nitrogen fluxes in arable land cultivation, but the approach lacks the explicit quantification of the different gaseous N fluxes. The study of Schroeck et al., (2019) overcame this hurdle and applied the process-based ecosystem model LandscapeDNDC to estimate the full regional nitrogen budgets including all fluxes of different ecosystems (cropland, grassland and pastures) and climatic zones of a water shed in Austria. That has been the first attempt estimating and reporting all the N fluxes possible as demanded by Gosz et al (2023).

The N balance estimate in Schroeck et al., (2019) for a catchment in Austria and the N balance reported in our study compares very well despite the inherent differences in land management and N inputs. As highlighted by Grosz et al., (2023), such intercomparisons demonstrate the different model behaviours when applied to different ecosystem. In our study, we see the partitioning of the N outfluxes from our arable system in similar shares as reported by Schroeck et al., (2019) for the arable land.

The N_2O estimate in Schroeck et al., (2019) and the current study is of a comparable level. We estimated N_2O emissions of 2.6 kg N ha^{-1} yr^{-1} while Schroeck et al., (2019) reports 1.51 kg N ha^{-1} yr^{-1}, about 40% lower. The NO fluxes differ significantly since we reported a mean value of 3.2 kg NO-N ha^{-1} yr^{-1} while Schroeck et al., (2019) reports 0.08 kg NO-N ha^{-1} yr^{-1}. This is on one hand related to some recent model advances, which have been made during this study, which elevated the NO production in LandscapeDNDC (Molina-Herrera et al., 2017) and on the other hand due to the high share of organic N fertilization in our study fostering NO emissions. Ammonia volatilization differs substantially between the two studies, while our study reports 34 kg NH_3-N ha^{-1} yr^{-1}, Schroeck et al., (2019) reported moderate emissions of 0.23 kg NH_3-N ha^{-1} yr^{-1}. The strong NH_3 volatilization in our study is mostly driven by the high pH-values of the soils in the region of Thessaly (pH values from 6.5 to 8.2 with a considerable

559 spatial variation, Greek Soil Map, 2015) and the comparable high manure inputs into the arable
560 system in our study, while in the research of Schroeck et al., (2019) the manure was preferably
561 applied only to the grassland systems and mineral fertilizers to the arable land. Concerning
562 the NO_3, Schroeck et al., (2019) reported 45.3 kg NO_3-N ha^{-1} yr^{-1} which was 3 times higher
563 compared to this study (14.1 kg N ha^{-1} yr^{-1}) considering the N-input of approximately 160 kg
564 and 212.3 kg N ha^{-1} yr^{-1} respectively. Even though 50 % or the arable land in our study was
565 irrigated, the resulting water percolation rates in our study were by far lower than the
566 percolation simulated in the study of Schroeck et al., (2019) as the Austrian pre-alpine
567 catchment received nearly double annual precipitation.
568 The N balance modelling study of Lee et al., (2020) was estimating for Switzerland a national
569 cropland N balance using an upscaling method based on process-based site simulations with
570 the DayCent model differentiating the management of the considered cropping systems e.g.
571 fertilizer rates, tillage or land cover change. The study reported for conventional cultivations
572 (averaged across 20 years) yield related N outfluxes accounting for about 60%, NO_3 leaching
573 36.1% and gaseous N emissions 4.1% of the total N outputs. Lee et al., (2020) did not report
574 the different gaseous N fluxes, even though the DayCent model must have simulated all of
575 them. Although the yield related N outflux is in accordance with our result of 64.95% there
576 seems to be a discrepancy in the reported gaseous and aquatic N fluxes contribution, as we
577 report 27.94% for gaseous and 7.11% for NO_3 leaching in our study. As demanded by Gosz
578 et al (2023) we can elaborate different preferences in simulated N outflux partitioning (36%
579 NO_3 and 4% gaseous losses for DayCent versus 7% NO_3 and 28% gaseous losses for
580 LandscapeDNDC) due to the different simulation models, regionalization and upscaling
581 approaches as well as due to the different soil, climatic and management conditions included
582 in the respective studies.
583 Velthof et al., (2009) used the MITTERA-EUROPE model/method, based on the concoction of
584 GAINS and CAPRI models, to estimate N fluxes of European soils on NUTS2 scale with the
585 use of European datasets and literature coefficients, where the fertilizer application and
586 management was similar to our methodology. The average N Input-Output balance was

587 calculated as 117 kg N ha^{-1} yr^{-1} composed by manure of 49 kg N ha^{-1} yr^{-1}, synthetic fertilizer of
588 58 kg N ha^{-1} yr^{-1} (in the current study for both cases 80.2 kg N ha^{-1} yr^{-1}), biological nitrogen
589 fixation of 2 kg N ha^{-1} yr^{-1} (our research 45.6 kg N ha^{-1} yr^{-1}) and N deposition of 7 kg N ha^{-1}
590 (current study 6.3 kg N ha^{-1} yr^{-1}). In contrast to our study the reported output fluxes for NH_3 of
591 8 kg NH_3-N ha^{-1} yr^{-1}, N_2O of 2 kg N_2O-N ha^{-1} yr^{-1}, NO_x of 2 kg NO_x-N ha^{-1} yr^{-1}, N_2 of 51 kg N_2-N
592 ha^{-1} yr^{-1} and NO_3 leaching of 7 kg NO_3-N ha^{-1} yr^{-1} while the differences with the results presented
593 in our study are NH_3 of 34.0 kg NH_3-N ha^{-1} yr^{-1}, N_2O of 2.6 kg N_2O-N ha^{-1} yr^{-1}, NO_x of 3.2 kg
594 NO_x-N ha^{-1} yr^{-1}, N_2 of 15.5 kg N_2-N ha^{-1} yr^{-1} and NO_3 leaching of 14.1 kg NO_3-N ha^{-1} yr^{-1}.
595 Additionally, the yield output is estimated as 48 kg N ha^{-1} yr^{-1}. Again, we see a different
596 preference in N outflux partitioning towards large shares in gaseous N fluxes versus small NO_3
597 leaching shares and the difference with the results presented in our study are related to the
598 different input data used for initialization and driving of the model, based on regional statistics
599 and the use of a biogeochemical model versus emission factor approaches.
600 He et al., (2018) assessed the soil N balance for a time spam between 1984 to 2014 based on
601 the N budget equations (N input – N output) using multiple coefficients from literature in order
602 to estimate the nitrogen input and output fluxes of six grouped regions in China. The used
603 datasets were acquired from national Authorities and include cropping land and yields,
604 synthetic fertilizers, animal heads, soil types etc. The N synthetic fertilizer input is in average
605 182.4 kg N ha^{-1} and the organic fertilizer of 97.3 kg N ha^{-1}, N fixation is estimated as 16.8 kg
606 N ha^{-1} and the atmospheric deposition as 22 kg N ha^{-1}. Almost half of the total averaged N
607 output losses, 48.9%, was attributed to crop uptake while the respective gaseous losses were
608 N_2 19.9%, volatilized NH_3 17.3%, N_2O 1.2% and NO 0.7%. As for the NO_3 leaching share was
609 5.8% of the total output N fluxes. These reported N outflux proportions comparable well to our
610 study. The differences in the N uptake data remain and are mainly due to the differences in
611 the crops and management.
612 As reported in OECD (OECD, 2020) the net averaged nitrogen balance of the area of our study
613 is 11.6 kg N ha^{-1} yr^{-1} input to the soil which corresponds very well to the simulated mean
614 nitrogen balance as an in-flux of 13.8 kg N ha^{-1} yr^{-1} (IQR 11.9 to 16.0) into the soil.

So far, the discussion of the presented N balance and N out fluxes compares well to most of the available studies reporting N balances while one modelling study report different N outflux partitioning between gaseous and NO_3 leaching fluxes. For more detailed intercomparison on the overall quality of our C and N fluxes we aim to compare our results versus various studies addressing individual components of the C and N balance and associated fluxes.

SOC stocks

Haas et al., (2022) reported results of a European inventory simulation of soil carbon stocks and N_2O emissions using a model ensemble. The study deployed in a baseline simulation across EU-27 a similar residues management as compared to our study resulting in very stable carbon stock dynamics over a long period (1950-2100). In this study, the estimated carbon sequestration of 0.5 (UA mean and median) $\pm$ 0.3 tons C ha^{-1} yr^{-1} is mainly caused by the inclusion of legume feed crops within the crop rotation leading to increased litter production and C input into the soil (Barneze et al., 2020; Fuchs et al., 2020; K. Petersen et al., 2021). Haas et al., (2022) reported a management scenario with 100% of crop litter remaining on the field leading to averaged C-sequestration rates of over 1 ton C ha^{-1} yr^{-1} across EU-27. As the residues management in this study is between the baseline and buried scenario of Haas et al., (2022), our results compare well to results reported in this study.

Other modelling studies such as (Lugato et al., 2014) reported C sequestration rates for the conversion of cropland into grassland ranging between 0.4 and 0.8 tons C ha^{-1} yr^{-1}. Lugato et al., (2014) reported averaged SOC change rates for a cereal straw incorporation scenario for EU-27 of 0.1 tons C ha^{-1} yr^{-1} (estimates from 2000 to 2020).

The SOC dynamics reported in this study show a stable carbon dynamic in the soil within the simulation time span (2009 - 2014) with only three years of model spin-up. The initialization of the various carbon pools with the SOC data from the soil database is balanced by the average litter production of the deployed crop rotations. The SOC increase in 2015 and 2016 is due to climatic conditions and higher litter inputs simulated by the model.

N_2O emissions

This study reported estimates of N_2O emissions of 2.6 ± 0.8 kg N_2O-N ha^{-1} yr^{-1} (IQR from 2.1 to 3.1) for a mixed crop / legume feed crop rotation, which were well above the estimates resulting from IPCC Tier I direct emission factors, IPCC would lead to 1.6 kg N_2O-N ha^{-1} yr^{-1} when applying 30pprox.. 160 kg N ha^{-1} yr^{-1}. The higher N_2O emission strength of the modelling is likely to result from emission peaks after irrigation due to low anaerobicity (Grosz et al., 2023; Janz et al., 2022). Cayuela et al., (2017) conducted a meta-analysis of the direct N_2O emissions for a number of cropping systems for the Mediterranean climate where the emission factors (Efs) were altered under different fertilization and irrigation conditions. Higher fertilization rates led to higher Efs (0.82% less than the 1% of IPCC). Additionally, irrigated and intensively cultivated crops had higher Efs than rainfed (up to 0.91% dependent on the irrigation method). The relatively high EF of maize in this study could be possibly attributed to the irrigation without the application of water-saving methods and the on average higher N application rates .

The LandscapeDNDC validation study of Molina-Herrera et al., (2016) reported for the Italian site Borgo Cioffi (Mediterranean climate, Ranucci et al., (2011) annual N_2O emissions of 2.49 kg N_2O-N ha^{-1} yr^{-1} while two sites in southern France showed annual N_2O emissions from 0.52 to 3.34 kg N_2O-N ha^{-1} yr^{-1}. N_2O emission estimates of our study were higher than results reported by Haas et al., (2022) using a multi model ensemble estimating average soil N_2O emissions from European (EU-27) cropping systems for the period 1980–1999 of 1.46 ± 1.30 kg N_2O-N ha^{-1} yr^{-1} under conventional (*Baseline*) management and comparable average N input. Klatt et al., (2015a) reported for an inventory (Saxony, Germany) mean N_2O emission of 1.43 ± 1.25 kg N_2O-N ha^{-1} yr^{-1}..

Overall, the reported N_2O flux component of our study compares well to the findings reported in literature. As critizised by Grosz et al. (2023), many studies only focus on the performance of the models in simulating N_2O emissions and the models were even calibrated for this purpose. Without reporting all the other N fluxes from the models, this

focusing and calibration for only one quantity can easily lead to inaccuracies for other components of the N cycle as they may not be checked for consistency anymore.

Janz et al., (2022)Janz et al., (2022)

Nitrate leaching

This study reported average NO_3 leaching fluxes (only nitrate leaching into surface waters) of 14.1 ± 4.5 kg NO_3-N ha^{-1} yr^{-1}. Reported nitrate leaching observations for the region or Greece could not be found in literatureestimated the NO_3 leaching with the use of four different models with varying values from 5 to 40 kg NO_3-N ha^{-1} yr^{-1} for the area of our study. These high values could be explained by the fact that it corresponds both to groundwater and runoff. Molina-Herrera et al., (2016) reported for the LandscapeDNDC validation study cropland nitrate leaching fluxes of approx. 7 to 88 kg NO_3-N ha^{-1} yr^{-1}. In addition, in the research of Molina-Herrera et al., (2017) the described NO_3 leaching results varied from 13 to 8 kg NO_3-N ha^{-1} yr^{-1} showing higher values in regards to the precipitation and fertigation. The most comparable site Borgo Cioffi resulted in a comparable annual NO_3 leaching flux of 18.62 kg NO_3-N ha^{-1} yr^{-1}.

Klatt et al., (2015b) reported in an uncertainty assessment for a regional inventory (Saxony, Germany) leaching rates of 29.32 ± 9.97 kg NO_3-N ha^{-1} yr^{-1} for a wheat-barley-rapeseed rotation simulated by the LandscapeDNDC model. The agricultural system and management regime is comparable; higher NO_3 leaching rates were most likely due to high N fertilization rates in combination with higher annual precipitation in the region leading to more intense percolation and therefore to stronger leaching of available NO_3 while in our study the fertilization regime was more lean such that soil nutrient competition was higher and available nitrate was more likely to be immobilized by plant uptake. Myrgiotis et al., (2019) reported in a similar assessment NO_3 leaching factor (LF) mean for their region of 14% (±7 %), in comparison we report mean NO_3 leaching factor of 7%.

NO emissions

In the current study, the model estimated NO emissions were in average 3.2 ± 1.5 kg NO-N ha^{-1} yr^{-1}. Butterbach-Bahl et al., (2009) performed the very first European inventory of soil NO emissions using a modified version of DNDC reporting low NO emission rates mostly below 2 kg NO-N ha^{-1} yr^{-1}. Molina-Herrera et al., (2017) recently reported a full NO emission inventory for the State of Saxony Germany compiling annual NO emissions from agricultural soils ranging from 0.19 to 6.7 kg NO-N ha^{-1} yr^{-1} simulated by LandscapeDNDC. The study reported the model performance on simulating soil NO emissions on more than 20 different sites. The study of Schroeck et al., (2019) reported for a regional inventory of arable soils in Austria simulated by LandscapeDNDC annual NO emissions of 1.0–1.5 kg NO-N ha^{-1} (for the year 2000), while empirical approaches such as Stehfest and Bouwman, (2006) estimated emission of similar magnitude. Zhang et al., (2015) reported in a model inter-comparison and validation study of NO and N_2O fluxes including three ecosystem models, consistent simulation results for the LandscapeDNDC model with NO emission strengths of cropland soils were between 1 and 3 kg NO-N ha^{-1} yr^{-1} across the sites.

NH_3 emissions

Schroeck et al., (2019) stated that validation studies of NH_3 volatilization for any biogeochemical model were very rarely reported in literature, mainly due to the complexity and a lack of flux observations at spatial and temporal high resolution.

In our study we estimate soil NH_3 emissions of 34.0 ± 6.7 kg NH_3-N ha^{-1} yr^{-1}. High NH_3 volatilization and emission rates can be explained by the predominating neutral to basal soils conditions (pH values of 7 and above) in the study region favouring the Henry NH_4/NH_3 equilibrium towards higher NH_3 gases enabling ammonia to diffuse out of the soil into the free atmosphere.

720 The IPCC emission factor (EF) method for NH_3 volatilization reports estimates of 20% of N
721 input into the soil to be volatilized as NH_3. For our study, IPCC methodology for NH_3 would
722 lead to 32 kg NH_3-N ha^{-1} yr^{-1}, which is well in line with the simulated result.
723 Sidiropoulos and Tsilingiridis, (2009) estimated a national livestock originated NH_3 emission
724 corresponding to approx. 22 kg ha^{-1} yr^{-1} for the region of Thessaly.
725 There is a number of national NH_3 inventories which could be considered detailed and well-
726 studied like the ones in Denmark, Netherlands, Europe, UK and US. In Denmark, (Geels et al.,
727 2012) used the DAMOS model to estimate the Danish NH_3 emissions (crop, grass and manure
728 manipulation) where the values ranged in the 5 regions under study from a very small quantity
729 to 17.4 kg NH_3-N ha^{-1} yr^{-1}.
730 As discussed by Sutton et al., (2013) the majority of the NH_3 emissions come as a result of the
731 agricultural production and are considerably impacted by climate influence. In the case of NH_3
732 volatilization, it could almost double every 5°C temperature given certain complex
733 thermodynamics dissociation and solubility, whilst soil NH_3 emission is influenced by the
734 available water quantity allowing the NH_x dissolution and use by microbial organisms, which is
735 afterwards leading to decomposition.
736
737

738 ## 4.3 Uncertainty Analysis and Quantification

739 Santabárbara, (2019) used the MCMC algorithm to estimate the joint parameter distribution of
740 the fundamental bio-geochemical process parameters in LandscapeDNDC when simulation
741 soil C and N fluxes. Propagating these joint parameter distributions through the model (by
742 sampling 500 joint parameter distributions and performing inventory simulations with each
743 parameter set with the model) for estimating the regional C and N fluxes was leading to various
744 distributions for any model result on the regional scale. Statistical analysis calculating mean,
745 median as well as the interquartile range (Q25 to Q75) determines best estimates and the
746 uncertainty range of any model output on the regional scale, demonstrating the superiority of

747 the method for assessing any ecosystem response by modelling instead of reporting single
748 results. This is a novel approach, that to our knowledge has not been reported before in
749 literature for the full carbon and nitrogen balance and neither been applied to regional
750 simulations by any process-based model.
751 In this study, the estimated UA mean and median of the carbon sequestration of 0.5 ± 0.3 tons
752 C ha^{-1} yr^{-1} is associated with an uncertainty range from 0.4 to 0.7 tons C ha^{-1} yr^{-1} which
753 compares well to the spatial uncertainty of C-sequestration in the study of Haas et al., (2022).
754 The approach used in this study enabled to assess the carbon and nitrogen balance of the
755 Lehuger et al., (2009b) used the Bayesian calibration method for the enhancement of the
756 CERES-EGC model parameterization (reduction of the apriori parameter distribution) as well
757 as quantification of the uncertainty of the simulated N_2O emissions in different sites. The
758 estimated fluxes of the different sites resulted in a range between 0.088 to 3.672 kg N_2O-N ha^{-1} yr^{-1} with values for the q05 quantile of 0.066 to 0.115 kg N_2O-N ha^{-1} yr^{-1} and for the Q95
760 quantile from 1.676 to 5.874 kg N_2O-N ha^{-1} yr^{-1} with an averaged value of 1.04 kg N_2O-N ha^{-1} yr^{-1} which is lower than the result of the current study but still in the same order of magnitude.
762 Klatt et al., (2015b) quantified a parameter-induced uncertainty analysis on the regional scale
763 applying the same process model for simulating N_2O emission and NO_3 leaching inventories
764 similar to our study. The region was represented by 4000 polygons of arable land (state of
765 Saxony, Germany) for crop rotations of barley, wheat and rapeseed while climatic conditions
766 differ. The results of Klatt et al., (2015b) display a likelihood range of 50% (the IQR range
767 between Q25 and Q75) for N_2O emissions from 0.46 to 2.05 kg N_2O-N ha^{-1} yr^{-1} which is in
768 good comparison to our results of 2.1 to 3.1 kg N_2O-N ha^{-1} yr^{-1}. The average N_2O emissions
769 are 1.43 kg N_2O-N ha^{-1} yr^{-1} comparable to the result of our study (mean: 2.6 and median: 2.5
770 kg N_2O-N ha^{-1} yr^{-1} across approx. 1000 polygons). As for leached NO_3, Klatt et al., (2015b)
771 reported leaching rates of mean value: 29 kg NO_3-N ha^{-1} yr^{-1}, (IQR from 24.5 to 36.0), which
772 is higher compared to the results of our study: Mean: 14.1 kg NO_3-N ha^{-1} yr^{-1}, median: 13.6
773 kg NO_3-N ha^{-1} yr^{-1} (IQR from 11 to 17). Despite the difference in climatic and soil conditions,

both uncertainty analysis studies reported similar regional estimates and uncertainty ranges for N_2O emissions and NO_3 leaching.

Butterbach-Bahl et al., (2022) reported the influence of management uncertainties for compiling national inventories of CH_4 and N_2O emission from various rice cultivation systems in Vietnam. The study applied a sampling technique varying model input data within a given range and analysing the influence on the assessed CH_4 and N_2O emission strengths. As the underlying cropland systems were fundamentally different, the assessed uncertainty ranges were comparable and the study is supporting our approach to focus on reporting uncertainty ranges rather than single values.

5 Conclusion

In this research, we presented for the first time a regional inventory of the full carbon and nitrogen balance including all sub-components of these fluxes simulated by a process-based model. Additionally, the study has fulfilled the demand to report always the associated uncertainties for any modelling results being published in literature. This supports the trustworthiness of the reported results for the C and N balances.

Comparing the modelled N balance with a similar approach modelling the full N balance with all associated fluxes for a catchment in pre-alpine Austria leads to the conclusion, that especially the partitioning the N outflux into the different N flux components is more inherent to the LandscapeDNDC model itself used in both studies than induced by the two very different agricultural and climatical systems. Nevertheless, specific N outfluxes between the two studies show large differences (e.g. NH_3 volatilization), which is purely caused by model processes due to different soil PH values. Comparing to a less granular and detailed study of the N balance for Switzerland gives a first impressions of the differences to be expected in modelling the arable N balance with various different models. The discussion of such results will become

more lively and maybe controversial as soon as more comparable studies using different models become available.

In addition, a full uncertainty analysis is presented based on the Metropolis-Hastings algorithm where a parameter subset and input data perturbation was sampled and simulated resulting in various probability density functions (PDF) for each one of the N and C balance fluxes building a full uncertainty analysis of the modelled results. This helps to build trustworthiness in modelling assessments and estimates of the balances as well as of the model behaviour.

As demanded by the nitrogen modelling community, all of the above constitute the novelty of the conducted research that could be seen as a prototype to analyse and report N cycling in agro-ecosystems in the future.

6 Aknowledgements

The author Odysseas Sifounakis received a Ph.D. research scholarship from Alexandros S. Onassis Public Benefit Foundation, Greece, part of which is the research presented in the current publication.

7 Code/Data availability

The LandscapeDNDC model source code is available via Butterbach-Bahl, Klaus; Grote, Rüdiger; Haas, Edwin; et al. (2021): LandscapeDNDC (v1.30.4). Karlsruhe Institute of Technology (KIT). DOI: 10.35097/438

All publication results (tables and data for figures) will be made available in the supplementary material associated with this paper.

8 Author contributions

Mr. Odysseas Sifounakis has conceived and designed the analysis and collected the data. He, also, performed the analysis and wrote the paper.

Dr. Edwin Haas conducted research and wrote the paper.

Prof. Dr. Klaus Butterbach-Bahl substantially contributed to research planning, manuscript writing and editing and, also, provided funding opportunities.

Prof. Dr. Maria P. Papadopoulou substantially contributed to research planning, manuscript writing and editing, and provided funding opportunities.

9 Competing interests

All authors have reviewed and accepted the submitted version and declare no conflicts of interest related to this publication.

10 References

Barneze, A.S., Whitaker, J., McNamara, N.P., Ostle, N.J., 2020. Legumes increase grassland productivity with no effect on nitrous oxide emissions. Plant Soil 446, 163–177. https://doi.org/10.1007/s11104-019-04338-w

Butterbach-Bahl, K., Baggs, E.M., Dannenmann, M., Kiese, R., Zechmeister-Boltenstern, S., 2013. Nitrous oxide emissions from soils: How well do we understand the processes and their controls? Philosophical Transactions of the Royal Society B: Biological Sciences. https://doi.org/10.1098/rstb.2013.0122

Butterbach-Bahl, K., Kahl, M., Mykhayliv, L., Werner, C., Kiese, R., Li, C., 2009. A European-wide inventory of soil NO emissions using the biogeochemical models DNDC/Forest-DNDC. Atmos Environ 43, 1392–1402. https://doi.org/10.1016/J.ATMOSENV.2008.02.008

Butterbach-Bahl, K., Kraus, D., Kiese, R., Mai, V.T., Nguyen, T., Sander, B.O., Wassmann, R., Werner, C., 2022. Activity data on crop management define uncertainty of CH 4 and N 2

O emission estimates from rice: A case study of Vietnam . Journal of Plant Nutrition and Soil Science. https://doi.org/10.1002/jpln.202200382

Camargo, J.A., Alonso, Á., 2006. Ecological and toxicological effects of inorganic nitrogen pollution in aquatic ecosystems: A global assessment. Environ Int. https://doi.org/10.1016/j.envint.2006.05.002

Cameron, D.R., van Oijen, M., Werner, C., Butterbach-Bahl, K., Grote, R., Haas, E., Heuvelink, G.B.M., Kiese, R., Kros, J., Kuhnert, M., Leip, A., Reinds, G.J., Reuter, H.I., Schelhaas, M.J., de Vries, W., Yeluripati, J., 2013. Environmental change impacts on the C- and N-cycle of European forests: A model comparison study. Biogeosciences 10, 1751–1773. https://doi.org/10.5194/bg-10-1751-2013

Cayuela, M.L., Aguilera, E., Sanz-Cobena, A., Adams, D.C., Abalos, D., Barton, L., Ryals, R., Silver, W.L., Alfaro, M.A., Pappa, V.A., Smith, P., Garnier, J., Billen, G., Bouwman, L., Bondeau, A., Lassaletta, L., 2017. Direct nitrous oxide emissions in Mediterranean climate cropping systems: Emission factors based on a meta-analysis of available measurement data. Agric Ecosyst Environ 238, 25–35. https://doi.org/10.1016/j.agee.2016.10.006

Chirinda, N., Kracher, D., Lægdsmand, M., Porter, J.R., Olesen, J.E., Petersen, B.M., Doltra, J., Kiese, R., Butterbach-Bahl, K., 2011. Simulating soil N2O emissions and heterotrophic CO2 respiration in arable systems using FASSET and MoBiLE-DNDC. Plant Soil 343, 139–160. https://doi.org/10.1007/s11104-010-0596-7

Ciais, P., Wattenbach, M., Vuichard, N., Smith, P., Piao, S.L., Don, A., Luyssaert, S., Janssens, I.A., Bondeau, A., Dechow, R., Leip, A., Smith, P.C., Beer, C., van der werf, G.R., Gervois, S., van oost, K., Tomelleri, E., Freibauer, A., Schulze, E.D., 2010a. The European carbon balance. Part 2: Croplands. Glob Chang Biol 16, 1409–1428. https://doi.org/10.1111/j.1365-2486.2009.02055.x

Ciais, P., Wattenbach, M., Vuichard, N., Smith, P., Piao, S.L., Don, A., Luyssaert, S., Janssens, I.A., Bondeau, A., Dechow, R., Leip, A., Smith, P.C., Beer, C., van der werf, G.R., Gervois, S., van oost, K., Tomelleri, E., Freibauer, A., Schulze, E.D., 2010b. The

879 European carbon balance. Part 2: Croplands. Glob Chang Biol 16, 1409–1428.
880 https://doi.org/10.1111/j.1365-2486.2009.02055.x
881 Dambreville, C., Morvan, T., Germon, J.C., 2008. N2O emission in maize-crops fertilized with
882 pig slurry, matured pig manure or ammonium nitrate in Brittany. Agric Ecosyst Environ
883 123, 201–210. https://doi.org/10.1016/j.agee.2007.06.001
884 Davidson, E.A., Kanter, D., 2014. Inventories and scenarios of nitrous oxide emissions.
885 Environmental Research Letters 9. https://doi.org/10.1088/1748-9326/9/10/105012
886 de Vries, W., Leip, A., Reinds, G.J., Kros, J., Lesschen, J.P., Bouwman, A.F., 2011.
887 Comparison of land nitrogen budgets for European agriculture by various modeling
888 approaches. Environmental Pollution 159, 3254–3268.
889 https://doi.org/10.1016/j.envpol.2011.03.038
890 del Grosso, S.J., Mosier, A.R., Parton, W.J., Ojima, D.S., 2005. DAYCENT model analysis of
891 past and contemporary soil N2O and net greenhouse gas flux for major crops in the USA.
892 Soil Tillage Res 83, 9–24. https://doi.org/10.1016/J.STILL.2005.02.007
893 del Grosso, S.J., Ogle, S.M., Nevison, C., Gurung, R., Parton, W.J., Wagner-Riddle, C., Smith,
894 W., Winiwarter, W., Grant, B., Tenuta, M., Marx, E., Spencer, S., Williams, S., 2022. A
895 gap in nitrous oxide emission reporting complicates long-term climate mitigation. Proc
896 Natl Acad Sci U S A 119. https://doi.org/10.1073/pnas.2200354119
897 del Grosso, S.J., Ojima, D.S., Parton, W.J., Stehfest, E., Heistemann, M., DeAngelo, B., Rose,
898 S., 2009. Global scale DAYCENT model analysis of greenhouse gas emissions and
899 mitigation strategies for cropped soils. Glob Planet Change 67, 44–50.
900 https://doi.org/10.1016/J.GLOPLACHA.2008.12.006
901 EFMA, 2009. SUSTAINABLE AGRICULTURE IN EUROPE.
902 Erisman, J.W., Galloway, J., Seitzinger, S., Bleeker, A., Butterbach-Bahl, K., 2011. Reactive
903 nitrogen in the environment and its effect on climate change. Curr Opin Environ Sustain
904 3, 281–290. https://doi.org/10.1016/J.COSUST.2011.08.012

ESDB, 2004. European Soil Database (ESDB) v2.0 - raster version [WWW Document]. URL https://esdac.jrc.ec.europa.eu/ESDB_Archive/ESDB/ESDB_Data/ESDB_v2_data_smu_1k.html (accessed 1.13.19).

EU-Commission, 2019. European Commission-Press release Nitrates: Commission decides to refer Greece to the Court of Justice and asks for financial sanctions.

EU-Commission, 2014. Tracking progress towards Kyoto and 2020 targets in Europe — European Environment Agency [WWW Document]. URL https://www.eea.europa.eu/publications/progress-towards-kyoto (accessed 1.13.19).

Franke, J.A., Müller, C., Elliott, J., Ruane, A.C., Jägermeyr, J., Balkovic, J., Ciais, P., Dury, M., Falloon, P.D., Folberth, C., François, L., Hank, T., Hoffmann, M., Izaurralde, R.C., Jacquemin, I., Jones, C., Khabarov, N., Koch, M., Li, M., Liu, W., Olin, S., Phillips, M., Pugh, T.A.M., Reddy, A., Wang, X., Williams, K., Zabel, F., Moyer, E.J., 2020. The GGCMI Phase 2 experiment: Global gridded crop model simulations under uniform changes in CO2, temperature, water, and nitrogen levels (protocol version 1.0). Geosci Model Dev 13, 2315–2336. https://doi.org/10.5194/gmd-13-2315-2020

Fuchs, K., Merbold, L., Buchmann, N., Bretscher, D., Brilli, L., Fitton, N., Topp, C.F.E., Klumpp, K., Lieffering, M., Martin, R., Newton, P.C.D., Rees, R.M., Rolinski, S., Smith, P., Snow, V., 2020. Multimodel Evaluation of Nitrous Oxide Emissions From an Intensively Managed Grassland. J Geophys Res Biogeosci 125. https://doi.org/10.1029/2019JG005261

Gabrielle, B., Laville, P., Hénault, C., Nicoullaud, B., Germon, J.C., 2006. Simulation of nitrous oxide emissions from wheat-cropped soils using CERES. Nutr Cycl Agroecosyst 74, 133–146. https://doi.org/10.1007/s10705-005-5771-5

Galloway, J.N., Leach, A.M., Bleeker, A., Erisman, J.W., 2013. A chronology of human understanding of the nitrogen cycle. Philosophical Transactions of the Royal Society B: Biological Sciences. https://doi.org/10.1098/rstb.2013.0120

Garnett, T., Appleby, M.C., Balmford, A., Bateman, I.J., Benton, T.G., Bloomer, P., Burlingame, B., Dawkins, M., Dolan, L., Fraser, D., Herrero, M., Hoffmann, I., Smith, P., Thornton,

933 P.K., Toulmin, C., Vermeulen, S.J., Godfray, H.C.J., 2013. Sustainable intensification in
934 agriculture: Premises and policies. Science (1979).
935 https://doi.org/10.1126/science.1234485
936 Geels, C., Andersen, H. v., Ambelas Skjøth, C., Christensen, J.H., Ellermann, T., Løfstrøm,
937 P., Gyldenkærne, S., Brandt, J., Hansen, K.M., Frohn, L.M., Hertel, O., 2012. Improved
938 modelling of atmospheric ammonia over Denmark using the coupled modelling system
939 DAMOS. Biogeosciences 9, 2625–2647. https://doi.org/10.5194/bg-9-2625-2012
940 Godfray, H.C.J., Beddington, J.R., Crute, I.R., Haddad, L., Lawrence, D., Muir, J.F., Pretty, J.,
941 Robinson, S., Thomas, S.M., Toulmin, C., 2010. Food security: The challenge of feeding
942 9 billion people. Science (1979). https://doi.org/10.1126/science.1185383
943 Grosz, B., Matson, A., Butterbach-Bah, K., Clough, T., Davidson, E.A., Dechow, R.,
944 Diamantopoulos, E., Dörsch, P., Haas, E., He, H., Henri, C. V, Hui, D., Well, R., Yeluripati,
945 J., Zhang, J., Scheer, C., 2023. Modeling denitrification: can we report what we don't
946 know? ESS Open Archive. https://doi.org/10.22541/essoar.168500283.32887682/v1
947 Grote, R., Lehmann, E., Brümmer, C., Brüggemann, N., Szarzynski, J., Kunstmann, H., 2009.
948 Modelling and observation of biosphere–atmosphere interactions in natural savannah in
949 Burkina Faso, West Africa. Physics and Chemistry of the Earth, Parts A/B/C 34, 251–260.
950 https://doi.org/10.1016/J.PCE.2008.05.003
951 Gurung, R.B., Ogle, S.M., Breidt, F.J., Williams, S.A., Parton, W.J., 2020. Bayesian calibration
952 of the DayCent ecosystem model to simulate soil organic carbon dynamics and reduce
953 model uncertainty. Geoderma 376. https://doi.org/10.1016/j.geoderma.2020.114529
954 Haas, E., Carozzi, M., Massad, R.S., Butterbach-Bahl, K., Scheer, C., 2022. Long term impact
955 of residue management on soil organic carbon stocks and nitrous oxide emissions from
956 European croplands. Science of The Total Environment 836, 154932.
957 https://doi.org/10.1016/J.SCITOTENV.2022.154932
958 Haas, E., Klatt, S., Fröhlich, A., Kraft, P., Werner, C., Kiese, R., Grote, R., Breuer, L.,
959 Butterbach-Bahl, K., 2013. LandscapeDNDC: A process model for simulation of

960 biosphere-atmosphere-hydrosphere exchange processes at site and regional scale.
961 Landsc Ecol 28, 615–636. https://doi.org/10.1007/s10980-012-9772-x
962 He, W., Jiang, R., He, P., Yang, J., Zhou, W., Ma, J., Liu, Y., 2018. Estimating soil nitrogen
963 balance at regional scale in China's croplands from 1984 to 2014. Agric Syst 167, 125–
964 135. https://doi.org/10.1016/J.AGSY.2018.09.002
965 Heinen, M., 2006. Application of a widely used denitrification model to Dutch data sets.
966 Geoderma 133, 464–473. https://doi.org/10.1016/J.GEODERMA.2005.08.011
967 Hénault, C., Bizouard, F., Laville, P., Gabrielle, B., Nicoullaud, B., Germon, J.C., Cellier, P.,
968 2005. Predicting in situ soil N2O emission using NOE algorithm and soil database. Glob
969 Chang Biol 11, 115–127. https://doi.org/10.1111/j.1365-2486.2004.00879.x
970 Holst, J., Grote, R., Offermann, C., Ferrio, J.P., Gessler, A., Mayer, H., Rennenberg, H., 2010.
971 Water fluxes within beech stands in complex terrain. Int J Biometeorol 54, 23–36.
972 https://doi.org/10.1007/s00484-009-0248-x
973 Houska, T., Kraft, P., Liebermann, R., Klatt, S., Kraus, D., Haas, E., Santabarbara, I., Kiese,
974 R., Butterbach-Bahl, K., Müller, C., Breuer, L., 2017. Rejecting hydro-biogeochemical
975 model structures by multi-criteria evaluation. Environmental Modelling and Software 93,
976 1–12. https://doi.org/10.1016/j.envsoft.2017.03.005
977 IFADATA [WWW Document], 2015. URL http://ifadata.fertilizer.org/ucSearch.aspx (accessed
978 1.13.19).
979 IPCC, 2019. 2019 Refinement to the 2006 IPCC Guidelines for National Greenhouse Gas
980 Inventories — IPCC [WWW Document]. URL https://www.ipcc.ch/report/2019-
981 refinement-to-the-2006-ipcc-guidelines-for-national-greenhouse-gas-inventories/
982 (accessed 1.12.19).
983 Jägermeyr, J., Müller, C., Ruane, A.C., Elliott, J., Balkovic, J., Castillo, O., Faye, B., Foster, I.,
984 Folberth, C., Franke, J.A., Fuchs, K., Guarin, J.R., Heinke, J., Hoogenboom, G., Iizumi,
985 T., Jain, A.K., Kelly, D., Khabarov, N., Lange, S., Lin, T.S., Liu, W., Mialyk, O., Minoli, S.,
986 Moyer, E.J., Okada, M., Phillips, M., Porter, C., Rabin, S.S., Scheer, C., Schneider, J.M.,
987 Schyns, J.F., Skalsky, R., Smerald, A., Stella, T., Stephens, H., Webber, H., Zabel, F.,

Rosenzweig, C., 2021. Climate impacts on global agriculture emerge earlier in new generation of climate and crop models. Nat Food 2, 873–885. https://doi.org/10.1038/s43016-021-00400-y

Janz, B., Havermann, F., Lashermes, G., Zuazo, P., Engelsberger, F., Torabi, S.M., Butterbach-Bahl, K., 2022. Effects of crop residue incorporation and properties on combined soil gaseous N2O, NO, and NH3 emissions—A laboratory-based measurement approach. Science of The Total Environment 807, 151051. https://doi.org/10.1016/J.SCITOTENV.2021.151051

Jones, C.M., Spor, A., Brennan, F.P., Breuil, M.C., Bru, D., Lemanceau, P., Griffiths, B., Hallin, S., Philippot, L., 2014. Recently identified microbial guild mediates soil N2O sink capacity. Nat Clim Chang 4, 801–805. https://doi.org/10.1038/nclimate2301

Kalivas, D., Kollias, V., Kalivas, D.P., Kollias, V.J., 2001. Effects of soil, climate and cultivation techniques on cotton yield in Central Greece, using different statistical methods 21. https://doi.org/10.1051/agro:2001110ï

Kasper, M., Foldal, C., Kitzler, B., Haas, E., Strauss, P., Eder, A., Zechmeister-Boltenstern, S., Amon, B., 2019. N 2 O emissions and NO 3− leaching from two contrasting regions in Austria and influence of soil, crops and climate: a modelling approach. Nutr Cycl Agroecosyst 113, 95–111. https://doi.org/10.1007/s10705-018-9965-z

Kim, Y., Seo, Y., Kraus, D., Klatt, S., Haas, E., Tenhunen, J., Kiese, R., 2015. Estimation and mitigation of N2O emission and nitrate leaching from intensive crop cultivation in the Haean catchment, South Korea. Science of The Total Environment 529, 40–53. https://doi.org/10.1016/J.SCITOTENV.2015.04.098

Klatt, S., Kraus, D., Rahn, K.-H., Werner, C., Kiese, R., Butterbach-Bahl, K., Haas, E., 2015a. Parameter-Induced Uncertainty Quantification of Regional N 2 O Emissions and NO 3 Leaching using the Biogeochemical Model LandscapeDNDC . pp. 149–171. https://doi.org/10.2134/advagricsystmodel6.2013.0001

Klatt, S., Kraus, D., Rahn, K.-H., Werner, C., Kiese, R., Butterbach-Bahl, K., Haas, E., 2015b. Parameter-Induced Uncertainty Quantification of Regional N 2 O Emissions and NO 3

1016 Leaching using the Biogeochemical Model LandscapeDNDC . pp. 149–171.
1017 https://doi.org/10.2134/advagricsystmodel6.2013.0001
1018 Kraus, D., Weller, S., Klatt, S., Haas, E., Wassmann, R., Kiese, R., Butterbach-Bahl, K., 2014.
1019 A new LandscapeDNDC biogeochemical module to predict CH4 and N2O emissions from
1020 lowland rice and upland cropping systems. Plant Soil 386, 125–149.
1021 https://doi.org/10.1007/s11104-014-2255-x
1022 Larocque, G.R., Bhatti, J.S., Boutin, R., Chertov, O., 2008. Uncertainty analysis in carbon cycle
1023 models of forest ecosystems: Research needs and development of a theoretical
1024 framework to estimate error propagation. Ecol Modell 219, 400–412.
1025 https://doi.org/10.1016/J.ECOLMODEL.2008.07.024
1026 Lee, K.M., Lee, M.H., Lee, J.S., Lee, J.Y., 2020. Uncertainty analysis of greenhouse gas
1027 (GHG) emissions simulated by the parametric Monte Carlo simulation and nonparametric
1028 bootstrap method. Energies (Basel) 13. https://doi.org/10.3390/en13184965
1029 Lehuger, S., Gabrielle, B., Oijen, M. van, Makowski, D., Germon, J.C., Morvan, T., Hénault,
1030 C., 2009a. Bayesian calibration of the nitrous oxide emission module of an agro-
1031 ecosystem model. Agric Ecosyst Environ 133, 208–222.
1032 https://doi.org/10.1016/j.agee.2009.04.022
1033 Lehuger, S., Gabrielle, B., Oijen, M. van, Makowski, D., Germon, J.C., Morvan, T., Hénault,
1034 C., 2009b. Bayesian calibration of the nitrous oxide emission module of an agro-
1035 ecosystem model. Agric Ecosyst Environ 133, 208–222.
1036 https://doi.org/10.1016/J.AGEE.2009.04.022
1037 Leip, A., Busto, M., Corazza, M., Bergamaschi, P., Koeble, R., Dechow, R., Monni, S., de
1038 Vries, W., 2011. Estimation of N 2O fluxes at the regional scale: Data, models, challenges.
1039 Curr Opin Environ Sustain. https://doi.org/10.1016/j.cosust.2011.07.002
1040 Li, C.S., 2000. Modeling trace gas emissions from agricultural ecosystems. Nutr Cycl
1041 Agroecosyst 58, 259–276.
1042 Li, X., Yeluripati, J., Jones, E.O., Uchida, Y., Hatano, R., 2015. Hierarchical Bayesian
1043 calibration of nitrous oxide (N2O) and nitrogen monoxide (NO) flux module of an agro-

ecosystem model: ECOSSE. Ecol Modell 316, 14–27. https://doi.org/10.1016/J.ECOLMODEL.2015.07.020

Lu, X., 2020. A meta-analysis of the effects of crop residue return on crop yields and water use efficiency. PLoS One 15. https://doi.org/10.1371/journal.pone.0231740

Lugato, E., Bampa, F., Panagos, P., Montanarella, L., Jones, A., 2014. Potential carbon sequestration of European arable soils estimated by modelling a comprehensive set of management practices. Glob Chang Biol 20, 3557–3567. https://doi.org/10.1111/gcb.12551

Lugato, E., Leip, A., Jones, A., 2018. Mitigation potential of soil carbon management overestimated by neglecting N2O emissions. Nat Clim Chang 8, 219–223. https://doi.org/10.1038/s41558-018-0087-z

Lyra, A., Loukas, A., 2021. Impacts of irrigation and nitrate fertilization scenarios on groundwater resources quantity and quality of the Almyros Basin, Greece. Water Supply 21, 2748–2759. https://doi.org/10.2166/ws.2021.097

Mavromatis, T., 2016. Spatial resolution effects on crop yield forecasts: An application to rainfed wheat yield in north Greece with CERES-Wheat. Agric Syst 143, 38–48. https://doi.org/10.1016/j.agsy.2015.12.002

Molina-Herrera, S., Grote, R., Santabárbara-Ruiz, I., Kraus, D., Klatt, S., Haas, E., Kiese, R., Butterbach-Bahl, K., 2015. Simulation of CO2 fluxes in European forest ecosystems with the coupled soil-vegetation process model “LandscapeDNDC.” Forests 6, 1779–1809. https://doi.org/10.3390/f6061779

Molina-Herrera, S., Haas, E., Grote, R., Kiese, R., Klatt, S., Kraus, D., Butterbach-Bahl, K., Kampffmeyer, T., Friedrich, R., Andreae, H., Loubet, B., Ammann, C., Horváth, L., Larsen, K., Gruening, C., Frumau, A., Butterbach-Bahl, K., 2017. Importance of soil NO emissions for the total atmospheric NOx budget of Saxony, Germany. Atmos Environ 152, 61–76. https://doi.org/10.1016/J.ATMOSENV.2016.12.022

Molina-Herrera, S., Haas, E., Klatt, S., Kraus, D., Augustin, J., Magliulo, V., Tallec, T., Ceschia, E., Ammann, C., Loubet, B., Skiba, U., Jones, S., Brümmer, C., Butterbach-Bahl, K.,

Kiese, R., 2016. A modeling study on mitigation of N2O emissions and NO3 leaching at different agricultural sites across Europe using LandscapeDNDC. Science of the Total Environment 553, 128–140. https://doi.org/10.1016/j.scitotenv.2015.12.099

Morris, M.D., 1991. Factorial Sampling Plans for Preliminary Computational Experiments, TECHNOMETRICS.

Musacchio, A., Re, V., Mas-Pla, J., Sacchi, E., 2020. EU Nitrates Directive, from theory to practice: Environmental effectiveness and influence of regional governance on its performance. Ambio 49, 504–516. https://doi.org/10.1007/s13280-019-01197-8

Myrgiotis, V., Rees, R.M., Topp, C.F.E., Williams, M., 2018a. A systematic approach to identifying key parameters and processes in agroecosystem models. Ecol Modell 368, 344–356. https://doi.org/10.1016/j.ecolmodel.2017.12.009

Myrgiotis, V., Williams, M., Rees, R.M., Topp, C.F.E., 2019. Estimating the soil N2O emission intensity of croplands in northwest Europe. Biogeosciences 16, 1641–1655. https://doi.org/10.5194/bg-16-1641-2019

Myrgiotis, V., Williams, M., Topp, C.F.E., Rees, R.M., 2018b. Improving model prediction of soil N2O emissions through Bayesian calibration. Science of the Total Environment 624, 1467–1477. https://doi.org/10.1016/j.scitotenv.2017.12.202

OECD, 2020. OECD (2020), Nutrient balance (indicator) [WWW Document]. URL https://data.oecd.org/agrland/nutrient-balance.htm (accessed 2.16.20).

Petersen, K., Kraus, D., Calanca, P., Semenov, M.A., Butterbach-Bahl, K., Kiese, R., 2021. Dynamic simulation of management events for assessing impacts of climate change on pre-alpine grassland productivity. European Journal of Agronomy 128, 126306. https://doi.org/10.1016/J.EJA.2021.126306

Petersen, R.J., Blicher-Mathiesen, G., Rolighed, J., Andersen, H.E., Kronvang, B., 2021. Three decades of regulation of agricultural nitrogen losses: Experiences from the Danish Agricultural Monitoring Program. Science of The Total Environment 787, 147619. https://doi.org/10.1016/J.SCITOTENV.2021.147619

1099 Portmann, F.T., Siebert, S., Döll, P., 2010. MIRCA2000-Global monthly irrigated and rainfed
1100 crop areas around the year 2000: A new high-resolution data set for agricultural and
1101 hydrological modeling. Global Biogeochem Cycles 24, n/a-n/a.
1102 https://doi.org/10.1029/2008gb003435
1103 Rahn, K.H., Werner, C., Kiese, R., Haas, E., Butterbach-Bahl, K., 2012. Parameter-induced
1104 uncertainty quantification of soil N 2O, NO and CO 2 emission from Höglwald spruce
1105 forest (Germany) using the LandscapeDNDC model. Biogeosciences 9, 3983–3998.
1106 https://doi.org/10.5194/bg-9-3983-2012
1107 Ramanantenasoa, M.M.J., Gilliot, J.M., Mignolet, C., Bedos, C., Mathias, E., Eglin, T.,
1108 Makowski, D., Génermont, S., 2018. A new framework to estimate spatio-temporal
1109 ammonia emissions due to nitrogen fertilization in France. Science of The Total
1110 Environment 645, 205–219. https://doi.org/10.1016/J.SCITOTENV.2018.06.202
1111 Ranucci, S., Bertolini, T., Vitale, L., di Tommasi, P., Ottaiano, L., Oliva, M., Amato, U., Fierro,
1112 A., Magliulo, V., 2011. The influence of management and environmental variables on soil
1113 N2O emissions in a crop system in Southern Italy. Plant Soil 343, 83–96.
1114 https://doi.org/10.1007/s11104-010-0674-x
1115 Ravishankara, A.R., Daniel, J.S., Portmann, R.W., 2009. Nitrous oxide (N2O): The dominant
1116 ozone-depleting substance emitted in the 21st century. Science (1979) 326, 123–125.
1117 https://doi.org/10.1126/science.1176985
1118 Refsgaard, J.C., van der Sluijs, J.P., Højberg, A.L., Vanrolleghem, P.A., 2007. Uncertainty in
1119 the environmental modelling process – A framework and guidance. Environmental
1120 Modelling & Software 22, 1543–1556. https://doi.org/10.1016/J.ENVSOFT.2007.02.004
1121 Robert, C., Casella, G., 2011. A short history of Markov Chain Monte Carlo: Subjective
1122 recollections from incomplete data. Statistical Science 26, 102–115.
1123 https://doi.org/10.1214/10-STS351
1124 Salteli, A., Tarantola, S., Campolongo, F., 2000. Sensitivity Analysis as an Ingredient of
1125 Modeling. Statistical Science 15, 377–395.

1126 Santabárbara, I., 2019. Analysis and quantification of parametric and structural uncertainty of
1127 the LandscapeDNDC model for simulating biosphere-atmosphere-hydrosphere
1128 exchange processes.
1129 Schroeck, A.M., Gaube, V., Haas, E., Winiwarter, W., 2019. Estimating nitrogen flows of
1130 agricultural soils at a landscape level – A modelling study of the Upper Enns Valley, a
1131 long-term socio-ecological research region in Austria. Science of the Total Environment
1132 665, 275–289. https://doi.org/10.1016/j.scitotenv.2019.02.071
1133 Sidiropoulos, C., Tsilingiridis, G., 2009. Trends of livestock-related NH3, CH4, N2O and PM
1134 emissions in Greece. Water Air Soil Pollut 199, 277–289. https://doi.org/10.1007/s11270-
1135 008-9877-7
1136 Smerald, A., Fuchs, K., Kraus, D., Butterbach-Bahl, K., Scheer, C., 2022. Significant Global
1137 Yield-Gap Closing Is Possible Without Increasing the Intensity of Environmentally Harmful
1138 Nitrogen Losses. Front Sustain Food Syst 6. https://doi.org/10.3389/fsufs.2022.736394
1139 Smith, P., Martino, D., Cai, Z., Gwary, D., Janzen, H., Kumar, P., McCarl, B., Ogle, S., O'Mara,
1140 F., Rice, C., Scholes, B., Sirotenko, O., Howden, M., McAllister, T., Pan, G., Romanenkov,
1141 V., Schneider, U., Towprayoon, S., Wattenbach, M., Smith, J., 2008. Greenhouse gas
1142 mitigation in agriculture. Philosophical Transactions of the Royal Society B: Biological
1143 Sciences. https://doi.org/10.1098/rstb.2007.2184
1144 Stehfest, E., Bouwman, L., 2006. N2O and NO emission from agricultural fields and soils under
1145 natural vegetation: Summarizing available measurement data and modeling of global
1146 annual emissions. Nutr Cycl Agroecosyst 74, 207–228. https://doi.org/10.1007/s10705-
1147 006-9000-7
1148 Sutton, M.A., Reis, S., Riddick, S.N., Dragosits, U., Nemitz, E., Theobald, M.R., Tang, Y.S.,
1149 Braban, C.F., Vieno, M., Dore, A.J., Mitchell, R.F., Wanless, S., Daunt, F., Fowler, D.,
1150 Blackall, T.D., Milford, C., Flechard, C.R., Loubet, B., Massad, R., Cellier, P., Personne,
1151 E., Coheur, P.F., Clarisse, L., van Damme, M., Ngadi, Y., Clerbaux, C., Skjøth, C.A.,
1152 Geels, C., Hertel, O., Kruit, R.J.W., Pinder, R.W., Bash, J.O., Walker, J.T., Simpson, D.,
1153 Horváth, L., Misselbrook, T.H., Bleeker, A., Dentener, F., de Vries, W., 2013. Towards a

climate-dependent paradigm of ammonia emission and deposition. Philosophical Transactions of the Royal Society B: Biological Sciences 368. https://doi.org/10.1098/rstb.2013.0166

Thomas, D., Johannes, K., David, K., Rüdiger, G., Ralf, K., 2016. Impacts of management and climate change on nitrate leaching in a forested karst area. J Environ Manage 165, 243–252. https://doi.org/10.1016/J.JENVMAN.2015.09.039

Thompson, R.L., Lassaletta, L., Patra, P.K., Wilson, C., Wells, K.C., Gressent, A., Koffi, E.N., Chipperfield, M.P., Winiwarter, W., Davidson, E.A., Tian, H., Canadell, J.G., 2019. Acceleration of global N2O emissions seen from two decades of atmospheric inversion. Nat Clim Chang 9, 993–998. https://doi.org/10.1038/s41558-019-0613-7

Tsakmakis, I.D., Kokkos, N.P., Gikas, G.D., Pisinaras, V., Hatzigiannakis, E., Arampatzis, G., Sylaios, G.K., 2019. Evaluation of AquaCrop model simulations of cotton growth under deficit irrigation with an emphasis on root growth and water extraction patterns. Agric Water Manag 213, 419–432. https://doi.org/10.1016/j.agwat.2018.10.029

Velthof, G.L., Oudendag, D., Witzke, H.P., Asman, W.A.H., Klimont, Z., Oenema, O., 2009. Integrated Assessment of Nitrogen Losses from Agriculture in EU-27 using MITERRA-EUROPE. J Environ Qual 38, 402–417. https://doi.org/10.2134/jeq2008.0108

Velthof, G.L., van Bruggen, C., Groenestein, C.M., de Haan, B.J., Hoogeveen, M.W., Huijsmans, J.F.M., 2012. A model for inventory of ammonia emissions from agriculture in the Netherlands. Atmos Environ 46, 248–255. https://doi.org/10.1016/J.ATMOSENV.2011.09.075

Vogeler, I., Giltrap, D., Cichota, R., 2013. Comparison of APSIM and DNDC simulations of nitrogen transformations and N2O emissions. Science of the Total Environment 465, 147–155. https://doi.org/10.1016/j.scitotenv.2012.09.021

Voloudakis, D., Karamanos, A., Economou, G., Kalivas, D., Vahamidis, P., Kotoulas, V., Kapsomenakis, J., Zerefos, C., 2015. Prediction of climate change impacts on cotton yields in Greece under eight climatic models using the AquaCrop crop simulation model

and discriminant function analysis. Agric Water Manag 147, 116–128. https://doi.org/10.1016/j.agwat.2014.07.028

Wagner-Riddle, C., Congreves, K.A., Abalos, D., Berg, A.A., Brown, S.E., Ambadan, J.T., Gao, X., Tenuta, M., 2017. Globally important nitrous oxide emissions from croplands induced by freeze-thaw cycles. Nat Geosci 10, 279–283. https://doi.org/10.1038/ngeo2907

Wang, G., Chen, S., 2012. A review on parameterization and uncertainty in modeling greenhouse gas emissions from soil. Geoderma 170, 206–216. https://doi.org/10.1016/J.GEODERMA.2011.11.009

Werner, C., Haas, E., Grote, R., Gauder, M., Graeff-Hönninger, S., Claupein, W., Butterbach-Bahl, K., 2012. Biomass production potential from Populus short rotation systems in Romania. GCB Bioenergy 4, 642–653. https://doi.org/10.1111/j.1757-1707.2012.01180.x

Zhang, W., Liu, C., Zheng, X., Zhou, Z., Cui, F., Zhu, B., Haas, E., Klatt, S., Butterbach-Bahl, K., Kiese, R., 2015. Comparison of the DNDC, LandscapeDNDC and IAP-N-GAS models for simulating nitrous oxide and nitric oxide emissions from the winter wheat–summer maize rotation system. Agric Syst 140, 1–10. https://doi.org/10.1016/J.AGSY.2015.08.003

Zistl-Schlingmann, M., Kwatcho Kengdo, S., Kiese, R., Dannenmann, M., 2020. Management Intensity Controls Nitrogen-Use-Efficiency and Flows in Grasslands—A 15N Tracing Experiment. Agronomy 10, 606. https://doi.org/10.3390/agronomy10040606

11 Appendix

11.1 Material and Methods

Sensitivity Index

In the first step, the Sensitivity Index algorithm (SI) (Pannell, 1997) was calculated for all process parameters by splitting the parameter ranges into 10 equidistant values from minimum to maximum and by rating SI values:

$$SI = \frac{CUM_{max} - CUM_{min}}{CUM_{max}}$$

where CUM_{max} and CUM_{min} are the maximum and minimum cumulative results of 10 simulations. High SI values explain a high sensitivity of the underlying parameter with respect to the model results, whereas low values or even zero indicates low or no sensitivity.

11.2 Results

Table A 1. Observed yield rates in the region of Thessaly. Cotton yields are the cotton bolls, clover feed is the total harvested above ground biomass, for wheat and barley it is the grain yield, maize is accounted grain ear and the stems Source ELSTAT.

Crop Yields [tons dry matter ha^{-1}]						
Crops	2012	2013	2014	2015	2016	Mean
Cotton	2.7	3.6	3.5	3.4	3.3	3.3
Clover	8.6	8.9	8.7	7.9	7.7	8.4
Wheat	3.3	3.3	3.3	3.7	3.6	3.4
Barley	3.2	3.2	3.2	3.5	3.5	3.3
Maize	10.9	12.1	12.3	12.7	12.1	12.0

Table A 2. Crop rotation scenarios (R1 – R5) for the region of Thessaly where the crop abbreviations corn, wiwh, perg, cott and wbar refer to maize, winter wheat, clover (legume feed crops s.a. alfalfa or vetch), cotton and winter barley respectively.

years	R1	R2	R3	R4	R5
2010	corn	wiwh	perg	cott	wbar
2011	wiwh	perg	cott	wbar	corn
2012	perg	cott	wbar	corn	wiwh
2013	cott	wbar	corn	wiwh	perg

2014	wbar	corn	wiwh	perg	cott
2015	corn	wiwh	perg	cott	wbar
2016	wiwh	perg	cott	wbar	corn

1220

1221 *Table A 3. Carbon Balance (totals) Summary of the Assessment and Uncertainty Analysis of the of cropland*
1222 *cultivation of the region of Thessaly, Greece, GPP gross primary productivity, TER terrestrial ecosystem respiration,*
1223 *Biomass export includes all C in yield, straw and feed exported from the fields, 360000 ha cropland.*

	Mean	Std	Median	Q25	Q75
	[mio. tons C yr^{-1}]	[mio. tons C yr^{-1}]	[mio. tons C yr^{-1}]	[mio. tons C yr^{-1}]	[mio. tons C yr^{-1}]
C-Inputs	4.51	0.20	4.45	4.36	4.69
C-Outputs	4.32	0.17	4.31	4.19	4.45
SOC-changes	0.19	0.11	0.20	0.14	0.27
Input fluxes					
GPP	4.25	0.20	4.21	4.11	4.42
C in manure	0.25	0.01	0.26	0.25	0.26
Output fluxes					
TER	3.08	0.16	3.06	2.97	3.20
Biomass export	1.24	0.05	1.24	1.21	1.27

1224

1225 *Table A 4 Nitrogen balance (totals) Summary of the Assessment and Uncertainty Analysis of the total Nitrogen*
1226 *Balance of cropland cultivation of the region of Thessaly, Greece.*

	Mean	Std	Median	Q25	Q75
	[kt-N yr^{-1}]	[kt-N yr^{-1}]	[kt-N yr^{-1}]	[kt-N yr^{-1}]	[kt-N yr^{-1}]
N-Inputs	76.5	3.2	77.8	73.3	79.1
N-Outputs	71.7	3.2	71.2	69.4	73.7
N-stock-changes	4.8	0.0	6.6	3.9	5.4
Input fluxes					
N deposition	2.0	0.3	2.1	1.9	2.1
Bio. N fixation	16.7	1.6	16.7	15.9	17.5
N in min. fertilizer	28.9	1.7	29.3	27.6	29.8
N in organic fertilizer	28.9	1.3	29.2	27.9	29.8

Output fluxes					
Gaseous emissions[1)]	21.2	3.1	21.1	18.9	23.4
N_2O	0.9	0.3	0.9	0.7	1.1
NO	1.1	0.5	1.0	0.7	1.4
N_2	4.9	2.4	4.5	2.9	6.6
NH_3	14.3	2.6	13.5	12.5	15.6
Aquatic fluxes[2)]					
NO_3 leaching	3.9	1.3	3.8	3.0	4.7

1) Gaseous emissions are the sum of N2O, NO, N2 and NH3 fluxes; 2) Aquatic flux is nitrate leaching (NO3-)

Table A 5. Total crop yields per cultivar and year.

Crop Yields [tons dry matter]						
Crops	2012	2013	2014	2015	2016	Mean
Cotton	303 676.9	374 424.6	359 806.7	322 292.0	285 780.3	329 196.1
Clover	302 753.2	319 401.7	338 134.6	341 938.4	360 693.9	332 584.4
Wheat	477 700.7	461 875.5	395 902.1	430 014.4	450 254.3	443 149.4
Barley	84 520.8	99 091.8	139 402.9	139 990.8	102 454.7	113 092.2
Maize	332 531.6	431 324.6	377 783.9	351 285.4	334 277.7	365 440.6

Figure 9. Shares of components of the annual nitrogen in- and output fluxes.

Table A 6. Simulated crop yields per cultivar and year for the irrigated land.

Crop Yields [tons dry matter ha^{-1}]

Crops	Median	Mean	STD
Cotton	4.0	3.7	0.9
Clover	9.8	9.6	0.6
Wheat	3.9	3.6	0.9
Barley	5.3	5.0	1.2
Maize	10.9	10.6	1.3

Table A 7. Simulated crop yields per cultivar and year for the rain feed land.

Crop Yields [tons dry matter ha^{-1}]			
Crops	Median	Mean	STD
Cotton	3.0	2.9	0.7
Clover	9.8	9.6	0.6
Wheat	3.9	3.6	0.9
Barley	4.0	3.9	0.9
Maize	9.5	9.2	1.5